https://dx.doi.org/10.1016/j.mbs.2025.109374

Highlights

Infection-induced host extinction: deterministic and stochastic models for environmentally transmitted pathogens

Bei Sun, Daozhou Gao, Xueying Wang, Yijun Lou

- This study identifies two crucial factors for a pathogen to lead to host extinction
- One is the pathogen's self-reproduction capacity in the environment; the other is the pathogen's impact on the fecundity and survival rates of the infected host
- These findings are theoretically supported by deterministic and stochastic modeling frameworks
- Deterministic model illustrates the existence and stability of equilibria based on certain threshold conditions involving three reproduction numbers: $\mathcal{R}_H$, $\mathcal{R}_B$, and $\mathcal{R}_0$
- Stochastic framework presents results on stochastic disease extinction, host population extinction, and the mean and variance for time to extinction
- Numerical simulations demonstrate host persistence, host extinction, extinction probability, and extinction time distributions, respectively

Infection-induced host extinction: deterministic and stochastic models for environmentally transmitted pathogens★

Bei Sun[a], Daozhou Gao[b], Xueying Wang[c] and Yijun Lou[a,*]

[a]Department of Applied Mathematics, The Hong Kong Polytechnic University, Hong Kong, China
[b]Department of Mathematics and Statistics, Cleveland State University, Cleveland, OH 44115, USA
[c]Department of Mathematics and Statistics, Washington State University, Pullman, WA 99164, USA

ARTICLE INFO

Keywords:
amphibian
host extinction
mathematical model
environmentally transmitted pathogens

ABSTRACT

Worldwide amphibian decline and extinction have been observed, highlighting the importance of identifying the underlying factors. This issue has long been recognized as highly significant and continues to receive substantial attention in conservation ecology. Pathogen infection, in particular the chytrid fungus *Batrachochytrium dendrobatidis*, is postulated as a key factor contributing to the decline of certain species within specific regions. In this paper, we focus on identifying the pathogen characteristics that can drive host species extinction. Both deterministic and stochastic modeling frameworks based on a susceptible-infectious-bacteria epidemic model are proposed, to assess the influence of pathogen infection on species decline and extinction. Various indices, including the reproduction numbers of the host species, the replication of the pathogen, and the transmission of the pathogen are derived. Theoretical analysis includes the stability of equilibria, the extinction and persistence of host species in the deterministic model, and the evaluation of extinction probability and average extinction time in the stochastic model. Additionally, numerical simulations are conducted to quantify the effects of various factors on host decline and extinction, as well as the probabilities of extinction. We find two crucial conditions for a pathogen to drive host extinction: (i) the pathogen's self-reproduction capacity in the environment, and (ii) the pathogen's impact on the fecundity and survival of the infected host. These findings provide insights that could aid in the design and implementation of effective conservation strategies for amphibians.

1. Introduction

Amphibian declines and extinctions have been observed globally and rapidly [47, 55, 59]. Reports indicate that out of 5743 described species, 32.5% are threatened. Since 1980, a minimum of 9 species, and potentially up to 122, have become extinct [47]. Compared to either birds or mammals, amphibians are facing a more rapid decline and are under greater threat [59]. Identifying the underlying factors contributing to these declines has long been recognized as a critical issue, continuing to draw significant attention in ecological research [7, 16, 27, 48, 55, 63]. These studies are crucial for the design and implementation of effective amphibian conservation strategies. They identify six primary factors contributing to modern amphibian declines: infectious diseases; climate change; changes in land use; commercial exploitation; the introduction of exotic species that compete with, prey on, or parasitize native frogs and salamanders; and contaminants. These factors may act alone or together.

Chytridiomycosis arises when the skin of a frog gets infected with the pathogenic chytrid fungus *Batrachochytrium dendrobatidis* (*Bd*), resulting in a catastrophic disruption of organism-wide metabolism, including the interruption of biosynthetic and degradative metabolic pathways, and significant dysregulation of cellular energy metabolism [28]. Following the emergence of the pathogen, numerous naive populations have experienced catastrophic declines or even extinction, and the persistence and transmission of the pathogen pose an ongoing threat to amphibian populations worldwide [1, 16, 62]. The primary focus of this study is to ascertain whether infectious diseases can solely drive host population extinction. If disease transmission can indeed lead to host extinction, we aim to further explore the underlying mechanisms contributing to such population extinction. These include the functional responses of pathogen transmission and reproduction within the host or the environment.

★Yijun Lou was supported in part by the NSF of China (12071393) and the General Research Fund from The Hong Kong Research Grants Council (15304821). Daozhou Gao was partially funded by the CSU Office of Research through a startup grant.

*Corresponding author
ORCID(s): 0000-0003-3864-2001 (.Y. Lou)

Numerous studies have been conducted to uncover the mechanisms of disease-induced extinction and assess the relative significance of these mechanisms in threatening natural populations [17, 30, 40, 56]. Key theoretical mechanisms proposed include: (i) the pronounced impact of small population sizes and stochastic events on extinction risk, exacerbated by disease outbreaks in endangered populations or the Allee effect, where low genetic variability facilitates pathogen invasion, diminishing population size and genetic diversity; (ii) the role of frequency-dependent transmission and non-uniform mixing in driving extinctions, with disease spread being influenced by the proportion of infected individuals rather than the total number of susceptible or infectious hosts [11]; (iii) the ability of generalist pathogens, including those with biotic and abiotic reservoirs, to overcome host density thresholds and cause extinction of a particular host species, with external reservoirs heightening extinction risk when external infection rates are high [52]; and (iv) the potential for indirect or trophic-mediated extinctions, where disease-induced declines or extinctions can trigger broader ecological consequences within the community [20]. However, simple deterministic models for specialist parasites with density-dependent transmission often fail to exhibit disease-induced extinction, as these models typically illustrate that parasites will go extinct before their hosts [17]. This study aims to propose a straightforward deterministic model with density-dependent transmission that predicts the disease-induced extinction, which offers additional mechanisms for this phenomenon.

Environmental factors, including floating pathogens, significantly influence the dissemination of the *Bd* fungus among frog populations [9, 13, 19, 31]. Transmission dynamics of infectious diseases with both host-to-host and environment-to-host transmission pathways have been extensively examined by mathematical models [2, 14, 15, 26, 35, 36, 37, 60, 68, 69]. Sun et al. [60] provided a thorough review on studies of multi-transmission routes, encompassing direct contact and environmental-mediated infection. Codeço [15] developed a model incorporating environmental factors, such as the concentration of *V. cholerae* in water, within an epidemiological framework. Ghosh et al. [26] explored a model that integrates vibrio concentration and environmental discharge density, which influences vibrio proliferation. Wang and Liao [68] proposed a deterministic model with nonlinear incidence rates and a generalized representation of pathogen levels in contaminated water, with the model's global dynamics subsequently analyzed using geometric and matrix-theoretic methods [14, 35], respectively. Despite these advances, the impact of the pathogen on host species extinction risk remains underexplored. Most existing models are disease-specific, focusing on the transmission dynamics of the pathogen, with little attention given to host persistence and extinction. This gap highlights the need for integrating disease transmission into models of host extinction risk.

To explore the mechanisms that determine the persistence or extinction of a host population within a host-pathogen interaction cycle, we will employ a compartmental modeling framework involving variables for numbers of susceptible and infected individuals, denoted by S and I respectively, as well as the concentration of the pathogen in the environment, denoted by B. Unlike traditional epidemiological models, which depict the transmission of infectious diseases as a process occurring when a susceptible host comes into direct contact with an infectious host, the compartment B allows us to incorporate an additional pathogen transmission route through an environment (reservoir) containing infectious agents deposited by infected hosts and accessed by recipient hosts [22]. Although the model formulation is primarily inspired by *chytridiomycosis* transmission in frogs, other diseases have also been described by the SIB compartmental models, such as bacterial (e.g., cholera [67] and brucellosis [60]), viral (e.g., avian influenza or hepatitis E in pigs), prion (e.g., chronic wasting disease), and parasitic (e.g., *cryptosporidium*) infections [22]. Various deterministic and stochastic models have been proposed to describe different mechanisms of disease transmission [4, 44, 45]. Unlike existing modeling studies that focus on the transmission dynamics, our aim is to examine the conditions that contribute to the potential decline and extinction of the host population. We will formulate and analyze two versions of the SIB epidemiological models. By examining the stability of various equilibria and uniform persistence of the deterministic model, we identify some important indices and the underlying mechanisms that lead to population extinction or persistence. The corresponding stochastic model is used to estimate the probabilities of disease extinction, major outbreaks, and host population extinction. Numerical simulations will be employed to verify the stability and persistence of the deterministic epidemic model, calculate the probability of disease extinction, simulate different sample paths of the continuous-time Markov chain (CTMC) model, and predict the time of extinction for the stochastic epidemic model. By integrating deterministic and stochastic approaches, we get a better understanding of potential factors that influence the persistence or extinction of host populations in the context of host-pathogen interactions with two types of transmission.

2. A deterministic model for environmentally transmitted pathogens

Let $S(t)$, $I(t)$ and $B(t)$ denote the population densities of susceptible hosts, infected hosts and the concentration of environmental pathogens, respectively. To keep the model simple while incorporating the direct transmission among hosts and indirect transmission between host and environment, we formulate the following model:

$$\begin{aligned} \frac{\mathrm{d}S(t)}{\mathrm{d}t} &= f_1(S(t)+\eta I(t))(S(t)+\eta I(t)) - d_N S(t) - \kappa B(t)S(t) - \beta\frac{S(t)I(t)}{1+\alpha I(t)}, \\ \frac{\mathrm{d}I(t)}{\mathrm{d}t} &= \kappa B(t)S(t) + \beta\frac{S(t)I(t)}{1+\alpha I(t)} - d_N I(t) - \mu I(t), \\ \frac{\mathrm{d}B(t)}{\mathrm{d}t} &= f_2(B(t))B(t) - d_B B(t) + \gamma I(t). \end{aligned} \tag{1}$$

The transmission routes between two-compartment hosts and environmental pathogens are illustrated in Figure 1. The birth functions $f_1(\cdot)$ and $f_2(\cdot)$ of the host and pathogen populations are assumed to take the Beverton-Holt form

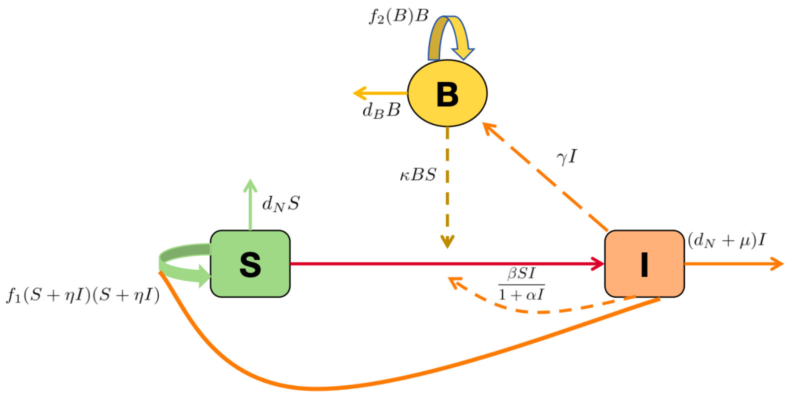

Figure 1: A schematic representation of host-pathogen transmission dynamics, incorporating both host-to-host and environment-to-host pathways.

[23, 39, 50, 66, 70], namely

$$f_1(x) = \frac{b_N}{1+\xi_N x} \quad \text{and} \quad f_2(x) = \frac{b_B}{1+\xi_B x}.$$

The parameter $\eta \in (0, 1]$ represents the reduced reproductivity of infected individuals [53, 58]. A susceptible host can become infected through direct contact with an infected host or exposure to an environmental pathogen with infection rates β and κ, respectively. Taking into account the impact of behavioral changes, we incorporate the Holling type II function into host-to-host transmission [24, 25, 43, 61]. Here, $\frac{1}{1+\alpha I}$ measures the inhibition effects resulting from the behavioral adaptations of susceptible individuals as the number of infected individuals increases, where α is a nonnegative constant. Furthermore, *Bd* possess the capability to reproduce independently at function $f_2(B(t))$ or be shed into the environment by infected individuals at rate γ. The inclusion of this term distinguishes our model from most existing studies. A summary of the model parameters and their corresponding descriptions is provided in Table 1.

It should be noted that model (1) aligns with the lifestyle framework of the second class of parasitic and saprophytic pathogens described in Lanzas et al. [34], which includes reproduction in the environment and environment-to-host transmission modes. For the reproduction of the host and pathogen populations and the pathogen transmission term, various functional forms have been proposed and fitted in modeling references. For illustrative purposes, in this study, the Beverton-Holt function is used to describe the host and bacteria proliferation, while the Holling type II functional response is adopted for the force of infection in the direct transmission route. Several discrete-time models commonly

Table 1
Parameter descriptions and baseline values.

Parameter	Description	Value	Reference
b_N	Background birth rate of hosts	0.55 day^{-1}	[51]
ξ_N	Crowding effect of host population	0.05 host^{-1}	Assumed
η	Reduced host reproduction due to infection	0.7	Assumed
d_N	Death rate of host population	0.05 day^{-1}	[29]
κ	Infection rate of a susceptible host by the environmental pathogen	0.0015 $\text{pathogen}^{-1}\text{day}^{-1}$	[19]
β	Infection rate of a susceptible host by an infected host	0.012 $\text{host}^{-1}\text{day}^{-1}$	[29]
α	Crowding effect of infected hosts	0.05 host^{-1}	Assumed
μ	Disease-induced death of an infected host	0.019 day^{-1}	[49]
b_B	Background birth rate of the pathogen	0.25 day^{-1}	[13]
ξ_B	Crowding effect of the pathogen	0.1 pathogen^{-1}	Assumed
d_B	Death rate of the pathogen	0.01 day^{-1}	[19]
γ	Release rate of the pathogen by an infected host	0.5 day^{-1}	[49]

utilize the Beverton-Holt function as a recruitment mechanism [39, 65, 66, 71]. Further functional forms can be found in the paper [34] in a general model for environmentally transmitted pathogens.

2.1. Well-posedness of the model

We first establish the well-posedness of the model (1), and the proof is postponed to Appendix A.

Proposition 2.1. *For each initial value* $(S(0), I(0), B(0)) \in \mathbb{R}^3_+$, *system (1) admits a unique solution* $(S(t), I(t), B(t)) \in \mathbb{R}^3_+$ *for all* $t \geq 0$. *Furthermore, the set*

$$\Omega = \left\{ (S, I, B) \in \mathbb{R}^3_+ \, : \, S + I \leq \frac{b_N}{\xi_N d_N} \text{ and } B \leq \frac{b_B}{\xi_B d_B} \right\}$$

is positively invariant.

2.2. Three reproduction numbers and summarized qualitative results

To simplify the presentation, we first introduce three biologically meaningful indices based on which some qualitative findings are established. Theoretical justifications for these results will be presented later.

We first check the host population growth model with no pathogen transmission ($I(t) = B(t) = 0$):

$$\frac{\mathrm{d}S(t)}{\mathrm{d}t} = \frac{b_N S(t)}{1 + \xi_N S(t)} - d_N S(t). \tag{2}$$

By using the idea in Fan et al. [21], we can introduce the net reproduction number for host population $\mathcal{R}_H := \frac{b_N}{d_N}$. For the scalar equation (2), it is easy to make the following conclusion.

Proposition 2.2. *The following statements are valid for system (2):*

(i) If $\mathcal{R}_H \leq 1$, *the trivial steady state* 0 *is global asymptotically stable;*

(ii) If $\mathcal{R}_H > 1$, *then there exists a unique positive steady state* $S_0 = \frac{1}{\xi_N}(\frac{b_N}{d_N} - 1) = \frac{1}{\xi_N}(\mathcal{R}_H - 1)$, *which is globally asymptotically stable in* $\mathbb{R}_+ \backslash \{0\}$.

Remark 2.1. The first two equations in (1) show that the total host population size $H(t) = S(t) + I(t)$ satisfies

$$\frac{dH(t)}{dt} \leq \frac{b_N H(t)}{1+\xi_N H(t)} - d_N H(t).$$

A simple comparison argument, combined with Proposition 2.2 (i) shows that the host population will go extinct as $\mathcal{R}_H \leq 1$.

If we ignore the shedding of pathogen from infectious hosts, then the dynamics of pathogen population are governed by

$$\frac{\mathrm{d}B(t)}{\mathrm{d}t} = \frac{b_B B(t)}{1+\xi_B B(t)} - d_B B(t). \tag{3}$$

Define the pathogen reproduction number in the habitat as $\mathcal{R}_B := \frac{b_B}{d_B}$. Similar to Proposition 2.2, we have the following conclusion.

Proposition 2.3. *The following statements are valid for system (3):*

(i) If $\mathcal{R}_B \leq 1$, the trivial steady state 0 is globally asymptotically stable;

(ii) If $\mathcal{R}_B > 1$, then there exists a unique positive steady state $B_0 = \frac{1}{\xi_B}(\frac{b_B}{d_B} - 1) = \frac{1}{\xi_B}(\mathcal{R}_B - 1)$, which is globally asymptotically stable in $\mathbb{R}_+\setminus\{0\}$.

When $\mathcal{R}_H > 1$ and $\mathcal{R}_B \leq 1$, we can introduce the basic reproduction number through the unique infection-free steady state $E_{10} = (S_0, 0, 0)$ of system (1) where $S_0 = \frac{1}{\xi_N}(\frac{b_N}{d_N} - 1)$. The new infection and transition matrices are given by:

$$F = \begin{pmatrix} \beta S_0 & \kappa S_0 \\ 0 & 0 \end{pmatrix} \text{ and } V = \begin{pmatrix} d_N + \mu & 0 \\ -\gamma & d_B - b_B \end{pmatrix}, \tag{4}$$

respectively. The next generation matrix of infection is

$$FV^{-1} = \begin{bmatrix} \frac{\beta S_0}{d_N+\mu} + \frac{\gamma\kappa S_0}{(d_N+\mu)(d_B-b_B)} & \frac{\kappa S_0}{d_B-b_B} \\ 0 & 0 \end{bmatrix},$$

and therefore, the basic reproduction number of model (1) can be defined as

$$\mathcal{R}_0 = \rho(FV^{-1}) = \frac{\beta S_0}{d_N+\mu} + \frac{\gamma\kappa S_0}{(d_N+\mu)(d_B-b_B)}.$$

The two terms in the above formula represent the secondary cases produced by direct contact and contaminated environment, respectively.

Based on these three reproduction numbers, $\mathcal{R}_H$, $\mathcal{R}_B$ and $\mathcal{R}_0$, we can establish the results as summarized in Table 2 and Figure 2 on the existence and local/global stability of all possible equilibria. It is interesting to observe from Table 2 and region E in Figure 2 that the host-free equilibrium $E_{01} = (0, 0, B_0)$ can retain locally stable even if $\mathcal{R}_H > 1$. This observation suggests the potential for host extinction in the event of disease spread. The proofs will be provided in the subsequent subsections.

2.3. Dynamical analysis of the deterministic model

This subsection is dedicated to the dynamical analysis of the model by providing theoretical arguments to those results reported in Table 2 and Figure 2.

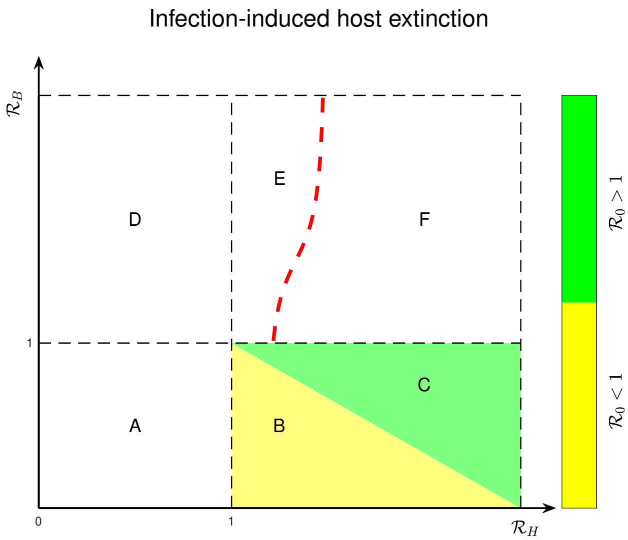

Figure 2: Partition areas based on the stability conditions of the equilibria. Region A: $E_{00} = (0, 0, 0)$ is globally asymptotically stable; Region B: $E_{10} = (S_0, 0, 0)$ is globally asymptotically stable; Regions C and F: the positive equilibrium $E^* = (S^*, I^*, B^*)$ exists; Regions D and E: $E_{01} = (0, 0, B_0)$ is locally stable. The red dashed line represents $b_N = \frac{(d_N+\kappa B_0)(d_N+\mu)}{\eta\kappa B_0+d_N+\mu}$.

Table 2
Existence and stability of equilibrium in system (1).

Equilibrium	Existence	Local stability	Global stability
$(0, 0, 0)$	Always exists	Locally stable if $\mathcal{R}_H < 1$ and $\mathcal{R}_B < 1$	Globally asymptotically stable
		Unstable if $\mathcal{R}_H > 1$ or $\mathcal{R}_B > 1$	
$(S_0, 0, 0)$	Exists if $\mathcal{R}_H > 1$	Locally stable if $\mathcal{R}_H > 1$, $\mathcal{R}_B < 1$ and $\mathcal{R}_0 < 1$	Globally asymptotically stable
		Unstable if $\mathcal{R}_H > 1$, but (i) $\mathcal{R}_B \geq 1$; or (ii) $\mathcal{R}_B < 1$ and $\mathcal{R}_0 > 1$	
	Does not exist if $\mathcal{R}_H \leq 1$		
$(0, 0, B_0)$	Exists if $\mathcal{R}_B > 1$	Locally stable if (i) $\mathcal{R}_B > 1$, $\mathcal{R}_H \leq 1$; or (ii) $\mathcal{R}_B > 1$, $d_N < b_N < \frac{(d_N+\kappa B_0)(d_N+\mu)}{\eta\kappa B_0+d_N+\mu}$	
		Unstable if $\mathcal{R}_B > 1$, $b_N > \frac{(d_N+\kappa B_0)(d_N+\mu)}{\eta\kappa B_0+d_N+\mu}$	
	Does not exist if $\mathcal{R}_B \leq 1$		
(S^*, I^*, B^*)	Exists if (i) $\mathcal{R}_H > 1$, $\mathcal{R}_B < 1$ and $\mathcal{R}_0 > 1$; or (ii) $\mathcal{R}_H > 1$, $\mathcal{R}_B > 1$ and $b_N > \frac{(d_N+\kappa B_0)(d_N+\mu)}{\eta\kappa B_0+d_N+\mu}$		
	Does not exist if (i) $\mathcal{R}_H \leq 1$, or (ii) $\mathcal{R}_H > 1$, $\mathcal{R}_B < 1$ and $\mathcal{R}_0 < 1$; or (iii) $\mathcal{R}_H > 1$, $\mathcal{R}_B > 1$ and $d_N < b_N < \frac{(d_N+\kappa B_0)(d_N+\mu)}{\eta\kappa B_0+d_N+\mu}$		

2.3.1. *The equilibrium* $E_{00} = (0, 0, 0)$

It is easy to see that system (1) always admits the trivial equilibrium $E_{00} = (0, 0, 0)$, where both hosts and pathogens are absent within the habitat. At this equilibrium, the Jacobian matrix takes the following form:

$$J\Big|_{E_{00}} = \begin{bmatrix} b_N - d_N & b_N\eta & 0 \\ 0 & -d_N - \mu & 0 \\ 0 & \gamma & b_B - d_B \end{bmatrix}.$$

Therefore, when $b_N - d_N > 0$ or $b_B - d_B > 0$ ($\mathcal{R}_H > 1$ or $\mathcal{R}_B > 1$), the equilibrium E_{00} is unstable.

Next, we investigate the case when $\mathcal{R}_H \leq 1$ and $\mathcal{R}_B \leq 1$. In this case, Remark 2.1 indicates that

$$\lim_{t\to\infty}(S(t), I(t)) = (0, 0).$$

Then the B-equation in system (1) is asymptotic to (3). Since $\mathcal{R}_B \leq 1$, we have $\lim\limits_{t\to\infty} B(t) = 0$ through the theory of asymptotically autonomous systems [57]. This shows that E_{00} is globally asymptotically stable when $\mathcal{R}_H < 1$ and $\mathcal{R}_B < 1$, implying that both hosts and pathogens will go extinct in this habitat under these conditions.

2.3.2. *The equilibrium* $E_{10} = (S_0, 0, 0)$

When $\mathcal{R}_H > 1$, the model (1) exhibits a disease-free equilibrium $E_{10} = (S_0, 0, 0)$ with $S_0 = \frac{1}{\xi_N}(\frac{b_N}{d_N} - 1)$. This equilibrium represents the infection-free state. Its stability can be argued through Appendix B and C, which is summarized as follows.

Proposition 2.4. *For model (1), if $\mathcal{R}_H > 1$, then the equilibrium $E_{10} = (S_0, 0, 0)$ exists. Furthermore,*

(i) this equilibrium is unstable if $\mathcal{R}_B \geq 1$, or $\mathcal{R}_B < 1$ and $\mathcal{R}_0 > 1$;

(ii) it is globally asymptotically stable if $\mathcal{R}_B < 1$ and $\mathcal{R}_0 < 1$.

2.3.3. *The equilibrium* $E_{01} = (0, 0, B_0)$

It is easy to see that system (1) admits the equilibrium $E_{01} = (0, 0, B_0)$ if and only if $\mathcal{R}_B > 1$. This equilibrium represents the state in the absence of the host population. Then we can conclude that E_{01} is locally stable if $b_N \leq d_N$ ($\mathcal{R}_H < 1$), or $d_N < b_N < \frac{(d_N+\kappa B_0)(d_N+\mu)}{\eta\kappa B_0+d_N+\mu}$. This equilibrium is unstable if $b_N > \frac{(d_N+\kappa B_0)(d_N+\mu)}{\eta\kappa B_0+d_N+\mu}$ (see Appendix D for a proof).

2.3.4. *Existence and uniqueness of the positive equilibrium*

This part is devoted to the study of the positive equilibrium. The proofs are given in Appendices E and F.

Proposition 2.5. *For system (1), if (i) $\mathcal{R}_H = \frac{b_H}{d_H} \leq 1$; or (ii) $\mathcal{R}_H > 1$, $\mathcal{R}_B < 1$ and $\mathcal{R}_0 < 1$; or (iii) $\mathcal{R}_B > 1$ and $d_N < b_N < \frac{(d_N+\kappa B_0)(d_N+\mu)}{\eta\kappa B_0+d_N+\mu}$, then there is no positive equilibrium.*

Proposition 2.6. *For system (1), if (i) $\mathcal{R}_H > 1$, $\mathcal{R}_B < 1$ and $\mathcal{R}_0 > 1$; or (ii) $\mathcal{R}_B > 1$ and $b_N > \frac{(d_N+\kappa B_0)(d_N+\mu)}{\eta\kappa B_0+d_N+\mu}$, then there is a positive equilibrium $E^* = (S^*, I^*, B^*)$. Moreover, the positive equilibrium is unique when it exists.*

2.4. Persistence of the pathogens and the host population

This subsection analyzes the persistence for the pathogens in the habitat and the host population. We first explore the trivial case when $\mathcal{R}_B > 1$. In this case, we have

$$\frac{\mathrm{d}B(t)}{\mathrm{d}t} \geq \frac{b_B B(t)}{1+\xi_B B(t)} - d_B B(t).$$

Then Proposition 2.3 and a comparison principle imply that

$$\liminf_{t\to\infty} B(t) \geq B_0 = \frac{1}{\xi_B}\left(\frac{b_B}{d_B} - 1\right) = \frac{1}{\xi_B}(\mathcal{R}_B - 1).$$

The case where $\mathcal{R}_H > 1$, $\mathcal{R}_B < 1$ and $\mathcal{R}_0 < 1$ has been studied in Proposition 2.4, which shows that the pathogen goes extinction. The subsequent result illustrates the persistence of pathogens in the habitat under the remaining scenario: $\mathcal{R}_H > 1$, $\mathcal{R}_B < 1$ and $\mathcal{R}_0 > 1$. The proof is given in Appendix G.

Theorem 2.1. *For system (1), if $\mathcal{R}_H > 1$, $\mathcal{R}_B < 1$ and $\mathcal{R}_0 > 1$, then the pathogen and host population uniformly persist, namely there exists a constant $\epsilon > 0$ such that any solution $(S(t), I(t), B(t))$ in $\mathbb{R}^3_+$ with $S(0) \geq 0, I(0) \geq 0, B(0) \geq 0$ satisfies $\liminf\limits_{t\to\infty}(I(t), B(t)) \geq (\epsilon, \epsilon)$.*

The next result also indicates the pathogen persistence in the habitat, but under a different scenario (refer to Appendix H for the proof). Note that in this case, $b_N > d_N$, i.e., $\mathcal{R}_H > 1$.

Theorem 2.2. *If $\mathcal{R}_B > 1$ and $b_N > \frac{(d_N+\kappa B_0)(d_N+\mu)}{\eta\kappa B_0+d_N+\mu}$, then the pathogen and host population uniformly persist, namely there exists a constant $\epsilon > 0$ such that any solution $(S(t), I(t), B(t))$ of the system (1) in $\mathbb{R}^3_+$ with $S(0) > 0$, $I(0) > 0$, $B(0) > 0$ satisfies $\liminf_{t\to\infty}(I(t), B(t)) \geq (\epsilon, \epsilon)$.*

2.5. Host extinction scenarios

This subsection focuses on examining the extinction and persistence of host population under specific scenarios.

2.5.1. No self-reproduction of the pathogen

We assume that the pathogens cannot reproduce by themselves, namely $b_B = 0$. In this case, the possibility of host population extinction is precluded, as shown in the next result with its proof presented in Appendix I.

Proposition 2.7. *For system (1), if $b_B = 0$ and $\mathcal{R}_H > 1$, then $\lim_{t\to\infty}(S(t) + I(t)) = 0$ does not hold for any solution $(S(t), I(t), B(t))$ in $\mathbb{R}^3_+$ with $S(0) > 0$, $I(0) \geq 0$, $B(0) \geq 0$.*

2.5.2. No impact of the pathogen on the hosts

We consider that the pathogen has no impact on the fecundity and survival of the hosts, namely $\eta = 1$ and $\mu = 0$. Then the total population $N(t) = S(t) + I(t)$ satisfies

$$\frac{\mathrm{d}N(t)}{\mathrm{d}t} = f_1(N(t))N(t) - d_N N(t),$$

which implies that

$$\lim_{t\to\infty} N(t) = \frac{1}{\xi_N}\left(\frac{b_N}{d_N} - 1\right) > 0$$

provided $\mathcal{R}_H = \frac{b_N}{d_N} > 1$. Consequently, the extinction of the host population driven solely by disease transmission is impossible.

The aforementioned observations demonstrate that the host population is persistent under certain conditions: (i) no pathogen self-replication, and (ii) pathogens do not affect host reproductivity or cause additional mortality. Conversely, pathogen-driven population extinction is possible upon two critical factors: (i) the pathogen's capacity to influence host fecundity or cause increased mortality, and (ii) the pathogen's ability to self-replicate within the environment. We will illustrate these observations through numerical simulations later.

3. Stochastic model for environmentally transmitted pathogens

Stochastic models incorporate the discrete transitions of individuals between epidemiological compartments, rather than the average transition rates between compartments [10]. In a stochastic epidemic model, numbers in each group are integers instead of continuously varying quantities. It is possible that the last infected individual could die or recover before the disease becomes endemic, and the disease can only reoccur if an infectious individual from outside the population is reintroduced [33, 44, 45]. In this section, we will propose a continuous-time Markov chain (CTMC) model, which is usually more realistic than our deterministic model [33].

We develop a CTMC model in line with the assumptions of the corresponding deterministic model (1) since the random variables related to the deterministic variables are discrete and time is continuous [42, 45]. For simplicity, we employ the same notations for the random variables and parameters as used in the deterministic model (1). Let time, $t \in [0, \infty)$, be continuous, and let $S(t)$, $I(t)$ and $B(t)$ denote the discrete-valued random variables for the numbers of susceptible hosts, infected hosts and environmental pathogens, respectively, with finite state space,

$$S(t), I(t) \in \{0, 1, 2, 3, \ldots, G_H\} \text{ and } B(t) \in \{0, 1, 2, 3, \ldots, G_B\},$$

where $G_H = \frac{b_N}{\xi_N d_N}$ and $G_B = \frac{b_B}{\xi_B d_B}$.

Table 3
State transitions and rates for the CTMC host-pathogen model

Event	Transition	Rate
Birth of host	$(S, I, B) \to (S + 1, I, B)$	$\frac{b_N(S+\eta I)}{1+\xi_N(S+\eta I)}$
Death of S	$(S, I, B) \to (S - 1, I, B)$	$d_N S$
Infection of host	$(S, I, B) \to (S - 1, I + 1, B)$	$(\kappa B + \frac{\beta I}{1+\alpha I})S$
Death of I	$(S, I, B) \to (S, I - 1, B)$	$(d_N + \mu)I$
Birth of pathogen	$(S, I, B) \to (S, I, B + 1)$	$\frac{b_B B}{1+\xi_B B}$
Release of pathogen	$(S, I, B) \to (S, I, B + 1)$	γI
Death of B	$(S, I, B) \to (S, I, B - 1)$	$d_B B$

The transition from one state to another may take place at any time t. Let $X(t) = \{S(t), I(t), B(t)\}$ and $\Delta X(t) = X(t + \Delta t) - X(t)$ for $t \geq 0$ and $\Delta t > 0$. By the Markov assumption, the waiting time between event transitions is exponentially distributed. For instance, the probability of the birth of a host in time Δt is given by

$$\mathbb{P}\left(\Delta X(t) = (1, 0, 0) | X(t)\right) = \frac{b_N(S(t) + \eta I(t))}{1 + \xi_N(S(t) + \eta I(t))} + o(\Delta t).$$

All state transitions and rates for the CTMC epidemic model are given in Table 3.

3.1. Stochastic disease extinction

The probabilities of disease extinction and invasion will be estimated by employing the theoretical framework of the Galton–Watson multitype branching process [3].

3.1.1. *Probability of disease extinction*

In the CTMC model, the disease spreads via two pathways: 1) infected hosts transmit the disease to susceptible hosts; 2) environmental pathogens infect susceptible hosts. Approximation of the nonlinear dynamics of CTMC model near the disease-free equilibrium leads to a multitype branching process in disease variables $I(t)$ and $B(t)$.

Let $P_{(i,b),(i+j_i,b+j_b)}(s, s+t)$ denote the transition probability of the process $\{Y(t) = (I(t), B(t))\}$ from $Y(s) = (i, b)$ to $Y(s+t) = (i+j_i, b+j_b)$ given $Y(s) = (i, b)$ for $s, t \geq 0$. Then we derive the backward Kolmogorov differential equation of the branching process approximation regarding (I, B) in Table 4. If initially there exists one single infected host, $I(0) = 1$, and no pathogen, $B(0) = 0$, then we define the offspring probability generating function (pgf) for infected host I as

$$y_1(u_1, u_2) = \frac{(d_N + \mu) + \beta S_0 u_1^2 + \gamma u_1 u_2}{d_N + \mu + \gamma + \beta S^*}. \tag{5}$$

The terms in (5) can be interpreted as follows: $\frac{\beta S_0}{d_N+\mu+\gamma+\beta S_0}$ represents the probability of disease transmission from an infected host to a susceptible host, resulting in one new infection. $\frac{\gamma}{d_N+\mu+\gamma+\beta S_0}$ specifies the probability that pathogen is shed by the infectious host resulting in one infectious host and one free-living pathogen in the environment. Lastly, $\frac{d_N+\mu}{d_N+\mu+\gamma+\beta S_0}$ corresponds to the probability of an infected host's death.

Likewise, the offspring pgf for B given that $I(0) = 0$ and $B(0) = 1$ can be derived as

$$y_2(u_1, u_2) = \frac{b_B u_2^2 + d_B + \kappa S_0 u_1 u_2}{b_B + d_B + \kappa S_0}. \tag{6}$$

In (6), the term $\frac{b_B}{b_B+d_B+\kappa S_0}$ denotes the probability of the birth of one environmental pathogen. The term $\frac{\kappa S_0}{b_B+d_B+\kappa S_0}$ represents the probability that the environmental pathogen successfully infects a susceptible host, resulting in one

Table 4
Transition probabilities of the branching process approximation for I and B

Event	Transition	Rate
Infection of host	$I \to I+1$	$(\kappa B + \beta I)S_0$
Death of I	$I \to I-1$	$(d_N + \mu)I$
Birth of pathogen	$B \to B+1$	$b_B B$
Release of pathogen	$B \to B+1$	γI
Death of B	$B \to B-1$	$d_B B$

newly infected host and keeping the original pathogen. The term $\frac{d_B}{b_B+d_B+\kappa S_0}$ gives the probability of the death of a single environmental pathogen.

Since the process $\{Y(t) : t \geq 0\}$ is time-homogeneous, we define $P_{(1,0),(0,0)}(s,t)$ and $P_{(0,1),(0,0)}(s,t)$ as $P_{(1,0)}(s)$ and $P_{(0,1)}(s)$ respectively. It follows from [6] that

$$\begin{aligned}\frac{\mathrm{d}P_{(1,0)}(s)}{ds} &= \left(\beta S_0 + d_N + \mu + \gamma\right)\left(P_{(1,0)}(s) - y_1\left(P_{(1,0)}(s), P_{(0,1)}(s)\right)\right),\\ \frac{\mathrm{d}P_{(0,1)}(s)}{ds} &= \left(\kappa S_0 + b_B + d_B\right)\left(P_{(0,1)}(s) - y_2\left(P_{(1,0)}(s), P_{(0,1)}(s)\right)\right),\end{aligned}$$

subject to the termination conditions $P_{(1,0)}|_{s=t} = P_{(0,1)}|_{s=t} = 0$, where $P_{(1,0)}$ and $P_{(0,1)}$ denote the functions of initial time s for any fixed termination time t.

Then the expectation matrix is

$$\mathbb{M} = \begin{bmatrix} \frac{\partial y_1(u_1,u_2)}{\partial u_1} & \frac{\partial y_2(u_1,u_2)}{\partial u_1} \\ \frac{\partial y_1(u_1,u_2)}{\partial u_2} & \frac{\partial y_2(u_1,u_2)}{\partial u_2} \end{bmatrix}_{u_1=1,u_2=1} = \begin{bmatrix} \frac{2\beta S_0+\gamma}{d_N+\mu+\gamma+\beta S_0} & \frac{\kappa S_0}{b_B+d_B+\kappa S_0} \\ \frac{\gamma}{d_N+\mu+\gamma+\beta S_0} & \frac{2b_B+\kappa S_0}{b_B+d_B+\kappa S_0} \end{bmatrix}.$$

By the Threshold Theorem in [5], $\rho(\mathbb{M}) < 1$ $(= 1, > 1)$ if and only if $\mathcal{R}_0 < 1$ $(= 1, > 1)$. Based on the theory of branching process [8, 18] and the Threshold Theorem, the probability of ultimate disease extinction is one if $\mathcal{R}_0 < 1$. When $\mathcal{R}_0 > 1$, the probability of ultimate disease extinction is determined by $\mathbb{P}_0 = q_1^{i_0} q_2^{b_0}$, where q_1 and q_2 are the fixed point of the probability generating functions on $(0,1)^2$ by setting $y_i(q_1,q_2) = q_i$, $i = 1,2$, and i_0 and b_0 are the initial numbers of infected hosts and environmental pathogens, respectively. That is,

$$\begin{aligned} y_1(q_1,q_2) &= \frac{(d_N+\mu) + \beta S_0 q_1^2 + \gamma q_1 q_2}{d_N + \mu + \gamma + \beta S_0} = q_1, \\ y_2(q_1,q_2) &= \frac{b_B q_2^2 + d_B + \kappa S_0 q_1 q_2}{b_B + d_B + \kappa S_0} = q_2. \end{aligned} \tag{7}$$

3.1.2. Mean and variance of disease extinction time

The mean and variance of disease extinction time can be investigated by the approach presented in [6]. Let $Y(t) = (I(t), B(t))$. Define

$$T = T_{(i_0,b_0)} = \inf\{t > 0 : I(t) = B(t) = 0 \ \text{ given } \ Y(0) = (i_0, b_0)\},$$

as the first time until disease extinction given $Y(0) = (i_0, b_0)$. Then the cumulative distribution function of T satisfies

$$\begin{aligned}\mathrm{P}(T \le t|T < \infty) &= \mathrm{P}\left(I(t) = B(t) = 0|T < \infty, Y(0) = (i_0, b_0)\right)\\ &= \frac{\mathrm{P}\left(I(t) = B(t) = 0|Y(0) = (i_0, b_0)\right)}{\mathrm{P}\left(T < \infty|Y(0) = (i_0, b_0)\right)} \approx \frac{P_{(i_0,b_0)}(t)}{\mathbb{P}_0},\end{aligned}$$

which implies that

$$\mathrm{P}(T \le t|T < \infty) \approx \frac{(P_{(1,0)}(t))^{i_0}(P_{(0,1)}(t))^{b_0}}{q_1^{i_0} q_2^{b_0}}.$$

Let $\Phi(i_0, b_0, t) = \mathrm{P}(T > t|T < \infty)$. The probability density of T is $-\frac{\partial \Phi(i_0,b_0,t)}{\partial t}$. Suppose that $\mathrm{E}(T) < \infty$, then the associated mean extinction time is given by

$$\begin{aligned}\mathrm{E}(T|T < \infty) &= -\int_0^\infty t\frac{\partial \Phi(i_0, b_0, t)}{\partial t}dt = \int_0^\infty \Phi(i_0, b_0, t)dt\\ &\approx \int_0^\infty \left[1 - \frac{(P_{(1,0)}(t))^{i_0}(P_{(0,1)}(t))^{b_0}}{q_1^{i_0} q_2^{b_0}}\right]dt,\end{aligned}$$

where integration by parts is applied and $\lim_{t\to\infty} t\Phi(i_0, b_0, t) = 0$. Similarly, the variance of the extinction time is

$$\begin{aligned}\mathrm{Var}(T|T < \infty) &= \mathrm{E}\left(T^2|T < \infty\right) - (\mathrm{E}(T|T < \infty))^2\\ &= \int_0^\infty 2t\Phi(i_0, b_0, t)dt - (\mathrm{E}(T|T < \infty))^2\\ &\approx \int_0^\infty 2t\left[1 - \frac{(P_{(1,0)}(t))^{i_0}(P_{(0,1)}(t))^{b_0}}{q_1^{i_0} q_2^{b_0}}\right]dt - \left\{\int_0^\infty \left[1 - \frac{(P_{(1,0)}(t))^{i_0}(P_{(0,1)}(t))^{b_0}}{q_1^{i_0} q_2^{b_0}}\right]dt\right\}^2\end{aligned}$$

provided that $\mathrm{E}(T^2) < \infty$.

3.2. Stochastic host population extinction

In the CTMC model, the presence of susceptible and infectious hosts in the system is accounted for by the reproduction of the host population and pathogen infection, respectively. Analogous to the stochastic disease model, we utilize the state transitions and rates in Table 3 to derive the offspring probability generating functions for the host population variables S and I. Specifically, assume that $\mathcal{R}_B > 1$ and we will approximate the CTMC model near the host-free steady state $(0, 0, B_0)$.

Similar to the above stochastic disease model, we acquire the backward Kolmogorov differential equation in terms of (S, I) based on the branching process approximation. Assuming an initial condition of a single susceptible host, $S(0) = 1$, and no infected individuals, $I(0) = 0$, the offspring pgf for the susceptible host S can be expressed as follows:

$$g_1(u_1, u_2) = \frac{b_N u_1^2 + d_N + \kappa B_0 u_2}{b_N + d_N + \kappa B_0}. \tag{8}$$

In (8), $\frac{b_N}{b_N+d_N+\kappa B_0}$ denotes the probability of the birth of one susceptible host; $\frac{d_N}{b_N+d_N+\kappa B_0}$ presents the probability of the death of one susceptible host and $\frac{\kappa B_0}{b_N+d_N+\kappa B_0}$ gives the probability that one susceptible host is infected by the pathogen and becomes an infected host.

Similarly, the offspring pgf for I can be derived under the conditions $S(0) = 0$ and $I(0) = 1$, as follows:

$$g_2(u_1, u_2) = \frac{b_N\eta \cdot u_1u_2 + d_N + \mu}{b_N\eta + d_N + \mu}. \tag{9}$$

In (9), $\frac{b_N\cdot\eta}{b_N\cdot\eta+d_N+\mu}$ gives the probability that one infected host gives birth to one susceptible host, which results in one infected host and one susceptible host in the population, and $\frac{d_N+\mu}{b_N\cdot\eta+d_N+\mu}$ represents the probability of the death of one infected host.

Similar to the expectation matrix $\mathbb{M}$ for disease extinction, we introduce the expectation matrix for host extinction

$$\mathbb{M}_p = \begin{bmatrix} \frac{\partial g_1(u_1,u_2)}{\partial u_1} & \frac{\partial g_2(u_1,u_2)}{\partial u_1} \\ \frac{\partial g_1(u_1,u_2)}{\partial u_2} & \frac{\partial g_2(u_1,u_2)}{\partial u_2} \end{bmatrix}_{u_1=1,u_2=1} = \begin{bmatrix} \frac{2b_N}{b_N+d_N+\kappa B_0} & \frac{b_N\cdot\eta}{b_N\cdot\eta+d_N+\mu} \\ \frac{\kappa B_0}{b_N+d_N+\kappa B_0} & \frac{b_N\cdot\eta}{b_N\cdot\eta+d_N+\mu} \end{bmatrix}.$$

According to the Threshold Theorem in [5], we conclude that the probability of population extinction in the CTMC model satisfies

$$\rho(\mathbb{M}_p) < 1\ (= 1, > 1 \text{ respectively }) \text{ if and only if } \ \rho(J_B) < 1\ (= 1, > 1 \text{ respectively}),$$

where

$$J_B = \begin{bmatrix} b_N - d_N - \kappa B_0 & b_N\eta \\ \kappa B_0 & -d_N - \mu \end{bmatrix}$$

corresponds to the Jacobian matrix of model (1) involving only variables S and I in the host-free steady state. Then we conclude that the probability of population extinction in the CTMC model satisfies

$$\rho(\mathbb{M}_p) < 1\ (= 1, > 1 \text{ respectively }) \text{ if and only if } \ \rho(J_B) < 1\ (= 1, > 1 \text{ respectively}).$$

It follows from the theory of branching process and the Threshold Theorem that the probability of ultimate host population extinction is one if $\rho(J_B) < 1$, which is consistent with the conclusion drawn from the deterministic model. For $\rho(\mathbb{M}_p) > 1$, there exists a fixed point of the offspring pgfs on $(0, 1)^2$, which gives the probability of host population extinction. We set the fixed point as $g_i(p_1, p_2) = p_i$, $p_i \in (0, 1)$, $\forall i = 1, 2$, where the values p_1 and p_2 are the probabilities of ultimate population extinction of susceptible and infected hosts respectively, which satisfies

$$g_1(p_1, p_2) = \frac{b_N p_1^2 + d_N + \kappa B_0 p_2}{b_N + d_N + \kappa B_0} = p_1,$$
$$g_2(p_1, p_2) = \frac{b_N\eta \cdot p_1p_2 + d_N + \mu}{b_N\eta + d_N + \mu} = p_2.$$

Then the probability of ultimate host extinction is given by $\mathbb{P}_0^H = p_1^{s_0} p_2^{i_0}$, where $S(0) = s_0$ and $I(0) = i_0$.

3.2.1. Mean and variance for time to host extinction

Let $H(t) = (S(t), I(t))$. Define

$$T^H = T^H_{(s_0,i_0)} = \inf\{t > 0 : S(t) = I(t) = 0 \ \text{ given } \ H(0) = (s_0, i_0)\},$$

as the first time instance of host extinction given $H(0) = (s_0, i_0)$. Then the cumulative distribution function of T^H satisfies

$$\begin{aligned} \mathrm{P}\left(T^H \le t | T^H < \infty\right) &= \mathrm{P}\left(S(t) = I(t) = 0 | T^H < \infty, H(0) = (s_0, i_0)\right) \\ &= \frac{\mathrm{P}\left(S(t) = I(t) = 0 | H(0) = (s_0, i_0)\right)}{\mathrm{P}\left(T^H < \infty | H(0) = (s_0, i_0)\right)} \approx \frac{P_{(s_0,i_0)}(t)}{\mathbb{P}_0^H}. \end{aligned}$$

It follows that

$$\mathrm{P}\left(T^H \le t | T^H < \infty\right) \approx \frac{(P_{(1,0)}(t))^{s_0}(P_{(0,1)}(t))^{i_0}}{p_1^{s_0} p_2^{i_0}}.$$

Let $\Psi(s_0, i_0, t) = \mathrm{P}\left(T^H > t | T^H < \infty\right)$. The probability density of T^H is $-\frac{\partial \Psi(s_0,i_0,t)}{\partial t}$. Suppose $\mathrm{E}(T^H) < \infty$. Then the associated mean extinction time is given by

$$\begin{aligned}\mathrm{E}\left(T^H | T^H < \infty\right) &= -\int_0^\infty t \frac{\partial \Psi(s_0, i_0, t)}{\partial t} dt = \int_0^\infty \Psi(s_0, i_0, t) dt \\ &\approx \int_0^\infty \left[1 - \frac{(P_{(1,0)}(t))^{s_0}(P_{(0,1)}(t))^{i_0}}{p_1^{s_0} p_2^{i_0}}\right] dt,\end{aligned}$$

where integration by parts is applied and $\lim_{t\to\infty} t\Psi(s_0, i_0, t) = 0$. By similar methods, the variance of host extinction time is given by

$$\begin{aligned}\mathrm{Var}\left(T^H | T^H < \infty\right) &= \mathrm{E}\left((T^H)^2 | T^H < \infty\right) - \left(\mathrm{E}\left(T^H | T^H < \infty\right)\right)^2 \\ &= \int_0^\infty 2t\Psi(s_0, i_0, t)dt - \left(\mathrm{E}\left(T^H | T^H < \infty\right)\right)^2 \\ &\approx \int_0^\infty 2t \left[1 - \frac{(P_{(1,0)}(t))^{s_0}(P_{(0,1)}(t))^{i_0}}{p_1^{s_0} p_2^{i_0}}\right] dt - \left\{\int_0^\infty \left[1 - \frac{(P_{(1,0)}(t))^{s_0}(P_{(0,1)}(t))^{i_0}}{p_1^{s_0} p_2^{i_0}}\right] dt\right\}^2\end{aligned}$$

provided that $\mathrm{E}((T^H)^2) < \infty$.

4. Numerical simulations

This section presents some numerical examples for the host-pathogen dynamics of the deterministic and stochastic models with parameter values in Table 1. The sample paths for the stochastic Markov chain model will be generated through the Gillespie algorithm [4].

Example 1 (Dynamical outcomes in the deterministic model). The existence and stability of each equilibrium, as outlined in Table 2, along with the corresponding partition areas depicted in Figure 2, are verified through a series of time-related simulations shown in Figure 3. Each subfigure illustrates the population sizes of the total hosts, infected hosts, and environmental pathogens as determined by the deterministic model under various scenarios and initial conditions. To simulate the existence and stability of the disease-free state, we set the parameters as follows: $b_B = 0.1$, $d_B = 0.75$, $\mu = 0.65$, and $b_N = 0.12$, with other parameter values specified in Table 1. Then $\mathcal{R}_H = 2.4 > 1$, $\mathcal{R}_B = 0.1333 < 1$, and $\mathcal{R}_0 = 0.4995 < 1$. Subfigure (a) demonstrates that all infections, including infected hosts and environmental pathogens, tend to become stably extinct, while the total host population persists stably. This outcome is consistent with Region B in Figure 2. To illustrate the host-free stability, we configure two sets of parameter values: (i) $b_N = 0.1$, $d_N = 0.15$, $d_B = 0.015$, $b_B = 0.06$ (then $\mathcal{R}_H = 0.667 < 1$ and $\mathcal{R}_B = 4 > 1$); and (ii) $b_N = 0.12$, $d_N = 0.1$, $d_B = 0.015$, $b_B = 0.15$ (therefore $\mathcal{R}_B = 10 > 1$ and $d_N < b_N < 0.131$). Additional parameter values are provided in Table 1. These configurations result in Subfigures (b) and (c), which show that both susceptible and infected host populations decrease to zero, while environmental pathogens stabilize at 30 and 90. This outcome occurs under conditions corresponding to Regions D and E in Figure 2, respectively. Subfigure (d) presents the existence of a positive equilibrium, denoted as $(S^*, I^*, B^*) = (15, 39, 104)$, with parameter values $b_B = 0.15$, $d_B = 0.2$, $b_N = 0.45$, and $d_N = 0.1$. This scenario aligns with Region C in Figure 2. These simulations elucidate four distinct scenarios concerning the existence and stability of equilibria, thereby validating the analytical results on the dynamics of each variable.

Example 2 (Host persistence). To explore the effects of no self-reproduction of the pathogen and no impact of the pathogen on the hosts, we choose the initial values $S(0) = 199$, $I(0) = 1$ and $B(0) = 0$ and the parameter values are set in Table 3. Figure 4 presents four sample paths of a stochastic epidemic model. These paths illustrate the

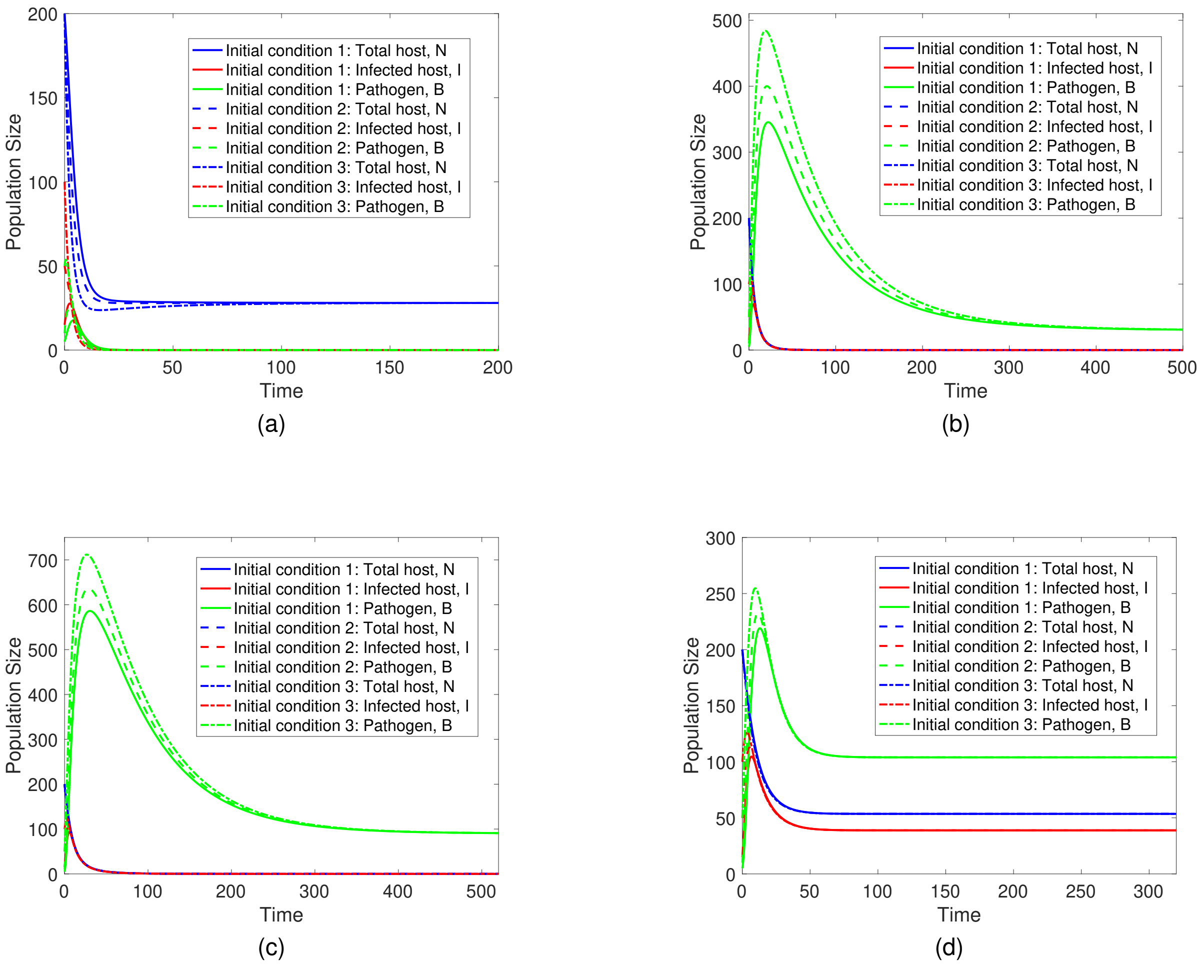

Figure 3: Population dynamics of the total host, infected host, and environmental pathogen in the deterministic model for various scenarios with diverse initial conditions. The initial conditions are specified as follows: (1.) $S(0) = 185, I(0) = 15, B(0) = 5$; (2.) $S(0) = 150, I(0) = 50, B(0) = 10$; (3.) $S(0) = 100, I(0) = 100, B(0) = 50$. Subfigure (a) illustrates the existence and stability of the disease-free equilibrium when $\mathcal{R}_H = 2.4 > 1$, $\mathcal{R}_B = 0.1333 < 1$, and $\mathcal{R}_0 = 0.4995 < 1$, corresponding to Region B in Figure 2. Subfigures (b) and (c) demonstrate the existence and stability of the host-free equilibrium under the conditions $\mathcal{R}_H = 0.667 < 1$ and $\mathcal{R}_B = 4 > 1$; and $\mathcal{R}_B = 10 > 1$ and $d_N < b_N < 0.131$, corresponding to Regions D and E in Figure 2, respectively. Subfigure (d) depicts the existence of the positive equilibrium with $\mathcal{R}_H = 4.5 > 1$, $\mathcal{R}_B = 0.75 < 1$, and $\mathcal{R}_0 = 15.882 > 1$, aligning with Region C in Figure 2.

dynamics of the total and infected host populations over time under different scenarios, alongside their corresponding deterministic solutions (dashed curves). In the first row, panels (a) and (b) depict a scenario with no self-reproduction of the pathogen population ($b_B = 0$). Panel (a) shows the total host population (N) starting around 200 and generally trending downward with notable fluctuations, while panel (b) illustrates the infected host population (I) initially spiking to around 200 before gradually declining. The stochastic paths in these panels reveal significant variability compared to the smoother deterministic solutions. In the second row, panels (c) and (d) represent a scenario where the pathogen does not affect reproduction and disease-induced mortality of infected individuals is zero ($\eta = 1$ and $\mu = 0$). Panel (c) indicates a more stable total host population with slight upward trends and high variability, starting around 200, whereas panel (d) shows the infected host population rapidly increasing to approximately 200 and then fluctuating with a slight upward trend. The deterministic solutions in these panels also provide smoother trends but do not capture the full variability seen in the stochastic paths. This simulation highlights the impact of pathogen

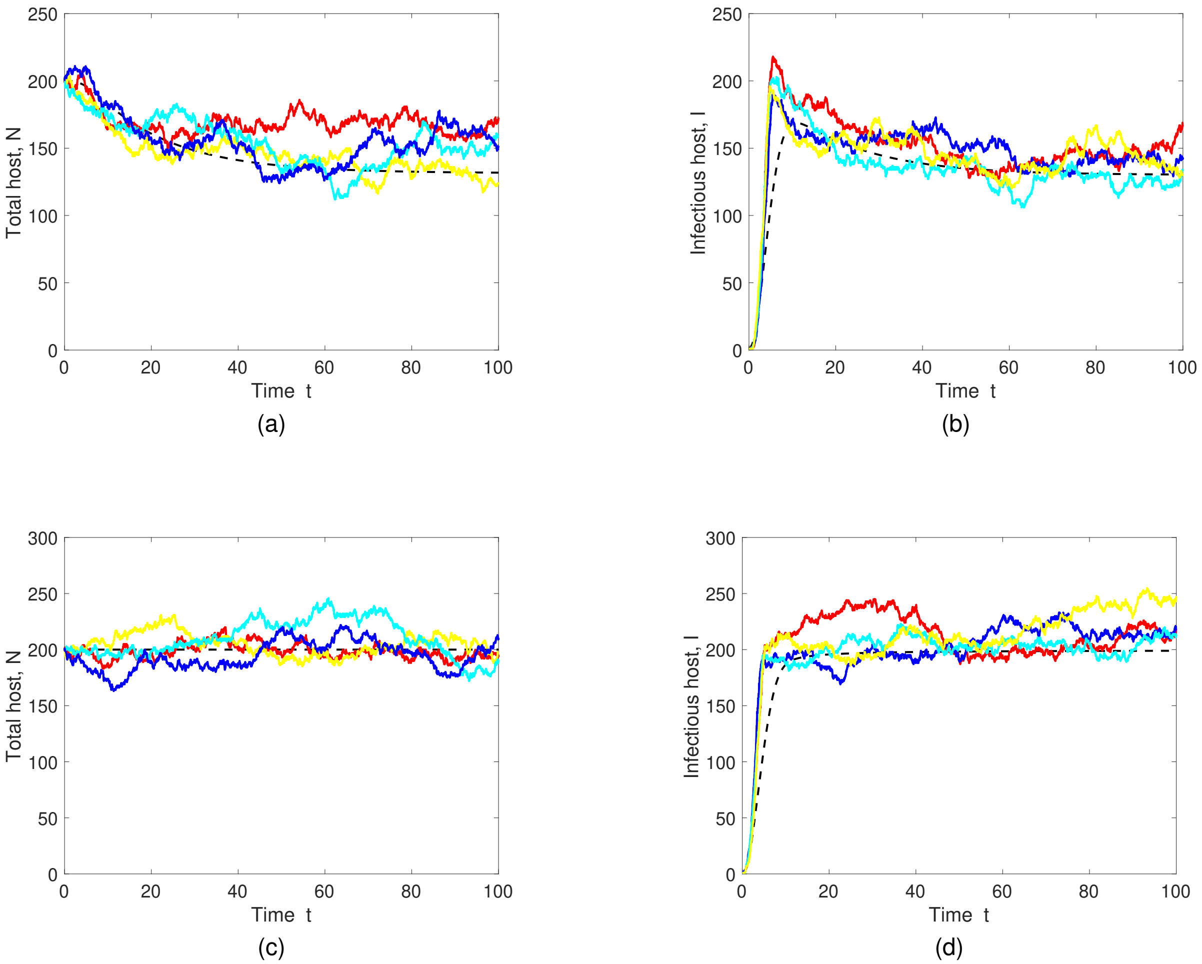

Figure 4: Four sample paths of the stochastic epidemic model for the total and infected hosts in both host and pathogen populations and the corresponding deterministic solution (dashed curve). The initial conditions are set as $S(0) = 199$, $I(0) = 1$ and $B(0) = 0$. The graphs (a) and (b) depict the scenario with no self-reproduction of pathogen population, namely $b_B = 0$, and other parameter values are shown in Table 1. Two graphs (c) and (d) present the scenario where the pathogen does not affect the reproduction and the disease-induced mortality of infected individuals, namely $\eta = 1$ and $\mu = 0$, and other parameter values are shown in Table 1.

reproduction and mortality on host population dynamics, demonstrating how different parameters can influence the spread and persistence of infections in host populations. Understanding these dynamics is crucial for designing effective interventions and managing epidemic outbreaks.

Example 3 (Host extinction). The reduced reproductive capacity of infected hosts may lead to host extinction. Figure 5 illustrates four sample paths of a stochastic epidemic model for different scenarios with reduced reproductive capacity of infected hosts. These paths compare the dynamics of the total and infected host populations over time with their corresponding deterministic solutions (dashed curves). Panels (a) and (b) in the first row depict the model using baseline parameters as specified in Table 1. Panel (a) shows the total host population (N), which starts around 200 and trends downward with notable variability among the stochastic paths, while the deterministic solution provides a smoother decreasing trend. Panel (b) displays the infected host population (I), which initially spikes to around 200 before declining with significant fluctuations, contrasted by a smoother decline in the deterministic solution. Panels (c) and (d) in the second row present a scenario with reduced reproduction among infected hosts due to the infection's impact ($\eta = 0.02$). Panel (c) indicates a more rapid decline in the total host population starting from around 200, shown

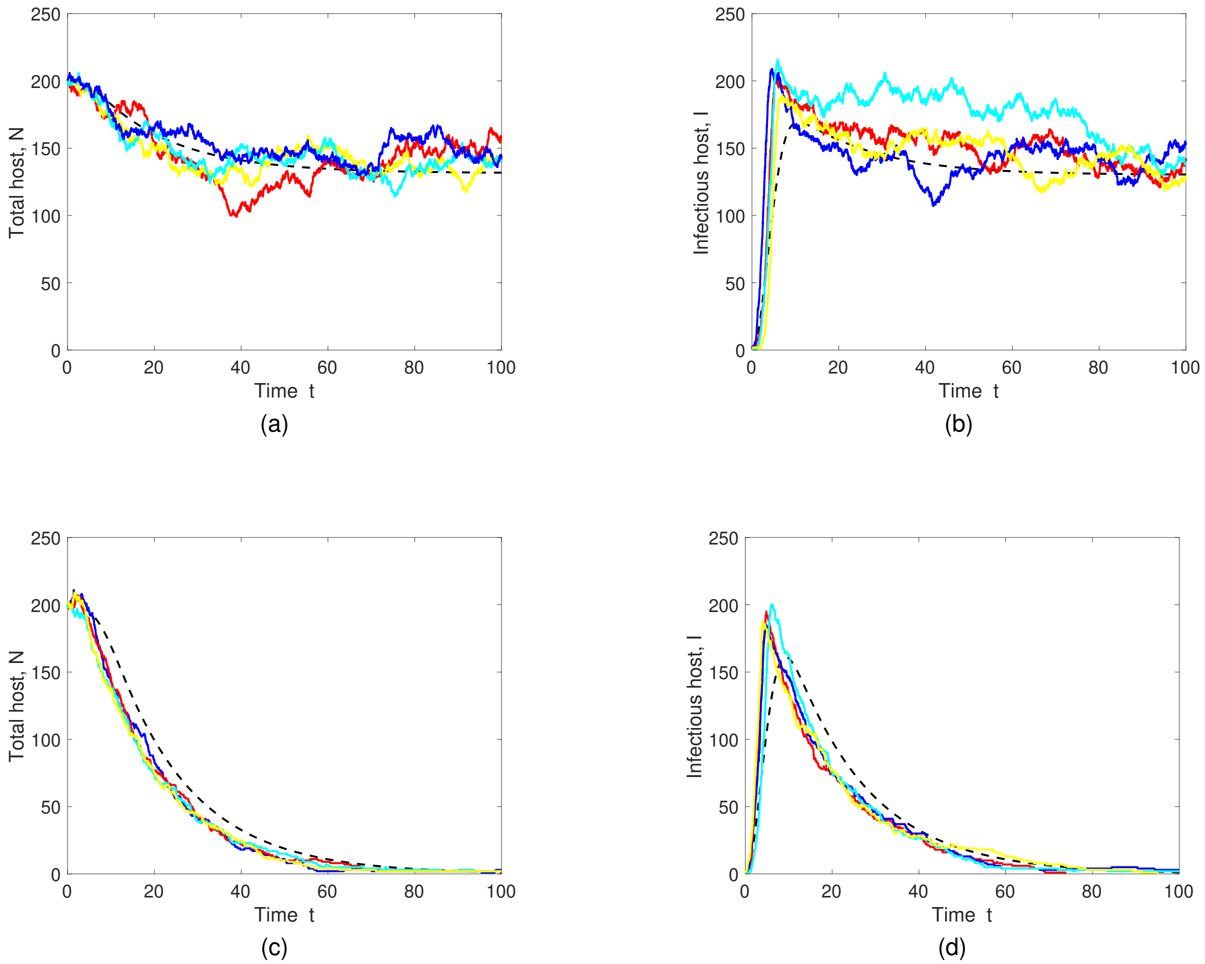

Figure 5: Four sample paths of the stochastic epidemic model for the total and infected hosts in both host and pathogen populations and the corresponding deterministic solution (dashed curve). The initial conditions are set as $S(0) = 199$, $I(0) = 1$ and $B(0) = 0$. The graphs (a) and (b) illustrate the model with parameter values from Table 1. The graphs (c) and (d) depict a scenario where there is limited reproduction among infected hosts due to the impact of the infection, namely $\eta = 0.02$, and other parameter values are shown in Table 1.

by the pronounced downward trend in both stochastic and deterministic paths. Panel (d) highlights the infected host population, which spikes to approximately 200 before a sharp decrease, as reflected in both the variable stochastic paths and the smoother deterministic solution. This analysis emphasizes the role of pathogen reproduction rates in shaping the persistence and extinction of host populations.

Example 4 (Extinction probability). The initial values of infected hosts and environmental pathogens impact disease extinction probability in the population. In Figure 6, we present the probability of disease extinction $\mathbb{P}_0$ as derived from the branching process model, considering varying initial sizes of infected hosts (i_0) and pathogens (b_0). These can be achieved by computing $q_1^{i_0} q_2^{b_0}$ with q_1 and q_2 determined by (7). Subfigure (a) indicates that the probability of disease extinction increases with smaller initial sizes of both infected hosts and pathogens. This is evidenced by the peak of the surface, which approaches $\mathbb{P}_0 = 1$ for low values of i_0 and b_0. The contour lines in subfigure (b) denote levels of constant extinction probability. It is observed that higher values of i_0 and b_0 correlate with higher extinction probabilities, reinforcing the conclusion that increasing initial numbers of infected hosts and environmental pathogens contribute positively to disease persistence. The probability of disease extinction is notably low when the disease is introduced by a few infected hosts, and it continues to decrease as the number of infected hosts increases. Conversely, if the disease originates from environmental pathogens with only a small initial count present at the onset of the epidemic, the probability of disease extinction is significantly high. Moreover, as the initial count of pathogens increases, the likelihood of a disease outbreak also rises. Therefore, the initial number of infected hosts poses a greater influence on the disease dynamics in this system during the early stages of the epidemic compared to the initial number of environmental pathogens. This behavior can be attributed to the scenario where a single infected host can release a larger quantity of environmental pathogens, which can subsequently infect more susceptible hosts, thereby diminishing the probability of disease extinction and amplifying the likelihood of a substantial disease outbreak.

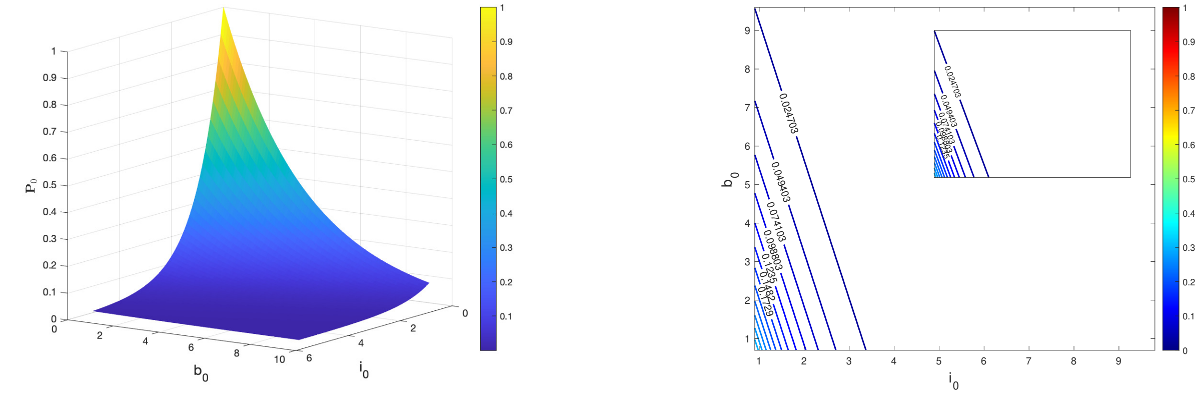

(a) (b)

Figure 6: Probability of disease extinction $\mathbb{P}_0$, solved from the branching process, for varying initial sizes of infected hosts and pathogens on (a) the 3D surface and (b) the contour plot with an inset. We set $b_N = 0.055$ day^{-1}, $\xi_N = 0.005$, $\beta = 1.2 \times 10^{-5}$ day^{-1} and $d_B = 0.245$ day^{-1}. Other parameter values are shown in Table 1.

Example 5 (Extinction time distribution of infection). To analyze the probability distribution of extinction times of infection under different initial conditions, we present the approximate probability distribution of extinction times for the number of infected individuals under varying initial conditions in Figure 7. In panel (a), where $S(0) = 50$, $I(0) = 1$ and $B(0) = 0$, the extinction time exhibits a pronounced peak around $0 - 1$ days with approximately 20% probability. This indicates that with only one initial infected individual and no environmental pathogens, the infection is likely to die out quickly, although there is a long tail extending up to 20 days suggesting occasional longer survival. Panel (b) with initial conditions $S(0) = 50$, $I(0) = 1$ and $B(0) = 1$ shows a similar peak but with a slightly lower probability. This suggests that the presence of one environmental pathogen marginally increases the infection persistence but does not significantly alter the extinction dynamics compared to panel (a). In panel (c), where $S(0) = 50$, $I(0) = 2$ and $B(0) = 0$, the extinction time distribution becomes more uniform with a peak around $1 - 3$ days and a tail extending to 25 days. This broader distribution indicates that with two initial infected individuals, the likelihood of infection persistence increases, thereby spreading the extinction times over a wider range. Finally, panel (d), which considers $S(0) = 50$, $I(0) = 10$ and $B(0) = 10$, displays a peak extinction time around $5 - 10$ days with a long tail reaching up to 40 days. The substantial increase in initial infected individuals and pathogens results in a significantly prolonged infection period. Overall, these simulations demonstrate that the initial number of infected individuals and environmental pathogens significantly impacts the extinction time distribution. Higher initial counts lead to longer infection durations due to increased transmission opportunities. All distributions exhibit a right-skewed pattern, indicating that while most infections extinguish quickly, a small number persist for extended periods.

5. Conclusion and discussion

Addressing the incidence of *Bd* pathogens in frog-inhabited regions poses substantial challenges in fighting against *chytridiomycosis* and in protecting frog populations. To contribute to these efforts, we incorporate the reproductive

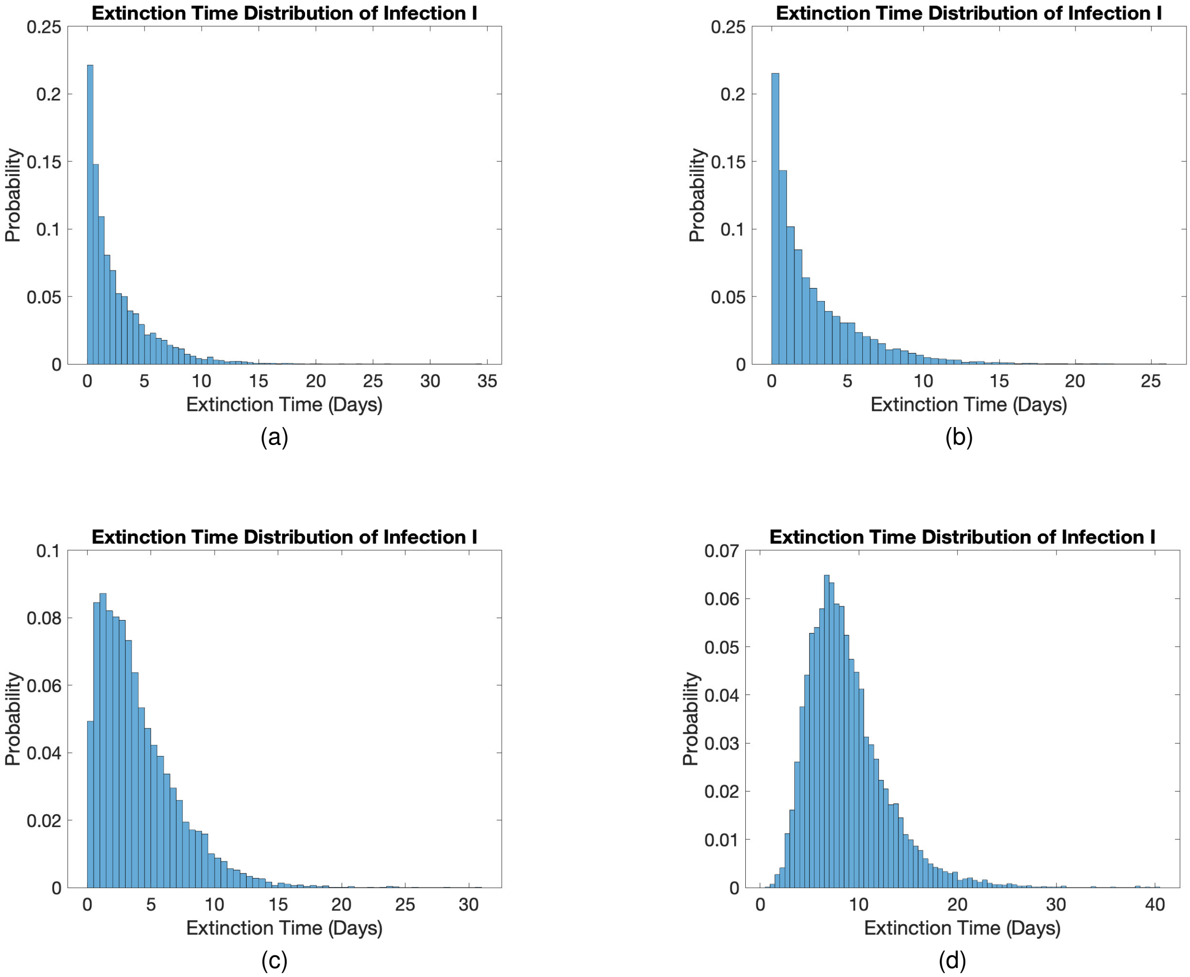

Figure 7: Approximate probability distribution of extinction time for the number of infected individuals with varying initial conditions: (a) $S(0) = 50$, $I(0) = 1$ and $B(0) = 0$; (b) $S(0) = 50$, $I(0) = 1$ and $B(0) = 1$; (c) $S(0) = 50$, $I(0) = 2$ and $B(0) = 0$; (d) $S(0) = 50$, $I(0) = 10$ and $B(0) = 10$. The parameter d_N is set to 0.55, and other parameter values are provided in Table 1.

mechanisms of frog and *Bd* pathogen populations, as well as their transmission pathways, into our model formulation. Both a deterministic model and its stochastic counterpart are constructed to illustrate the interplay among susceptible hosts, infectious hosts, and environmental pathogens. The model includes two transmission routes: direct transmission between susceptible and infected hosts, and indirect transmission of susceptible hosts by environmental pathogens. Environmental pathogens can reproduce independently and can also be released by infectious hosts. Furthermore, these pathogens may induce additional disease-induced mortality in infected hosts or reduce the fertility of these hosts. Additionally, we explore host-associated mechanisms for persistence and tolerance.

Theoretically, we confirm the well-posedness of the deterministic model by showing the existence, uniqueness, positivity, and boundedness of the solutions. Subsequently, we investigate the dynamics of the model system by three associated threshold parameters: the net reproduction number of the host population $\mathcal{R}_H$, the pathogen reproduction number $\mathcal{R}_B$, and the basic reproduction number of the infection $\mathcal{R}_0$. We determine the global stability of the disease-free and host-free equilibria, in addition to the uniform persistence under two sets of biologically interpretable conditions. Furthermore, we identify two scenarios under which the host population persists: one where the pathogens do not reproduce, and the other where the pathogen has no impact on the host population. These theoretical results partially align with the persistence mechanisms proposed by Brannelly et al. [12], such as enhanced host tolerance and effective pathogen attenuation, both of which contribute to reducing the pathogen's impact on the host population and increasing host survival and persistence. Other persistence mechanisms merit verification in future research. In practical applications, we can calibrate the parameters of the deterministic model using data from specific habitats to calculate the corresponding threshold reproduction numbers. Based on the dynamical conditions derived from theoretical analysis, we can then assess the existence and stability of the host and pathogen equilibria. This information allows us to implement targeted intervention and management strategies to maintain the ecological balance of amphibians.

Although the extinction threshold in the deterministic model provides valuable insights into the potential extinction of the disease and host, the likelihood of these events would also be interesting. For that purpose, a stochastic continuous-time Markov chain model is constructed on the foundation of a deterministic model. This is accomplished by utilizing the theory of the multitype branching process, which is particularly relevant when there are only a few infected individuals at the beginning of an epidemic, a scenario that cannot be effectively addressed by a deterministic model. In the stochastic model, we apply the multitype branching process theory for both (I, B) and (S, I) to estimate the probabilities of disease and host population extinction, respectively. Analytical and numerical results demonstrate that the probabilities of disease and host population extinction, denoted as $\mathbb{P}_0$ and $\mathbb{P}_0^H$, obtained from the multitype branching process theory, align remarkably well with the numerically approximated probabilities derived from a proportion of sample paths that lead to zero before an outbreak occurs. In practice, empirical data on initially infected individuals can be utilized to approximate the probability of disease extinction and the probability distribution of extinction time, which are crucial for informing interventions and management strategies aimed at maintaining ecological balance.

Numerical simulations verify the existence and stability of equilibria as shown in Figure 3. Additionally, they illustrate four sample paths of the stochastic epidemic model for the total and infected hosts under different scenarios: no self-reproduction of the pathogen, no impact of the pathogen on the hosts, and reduced reproduction of infected hosts. The results indicate that the host population is persistent under conditions of no self-reproduction of the pathogen or no impact of the pathogen on the hosts, while the host population goes extinct under reduced fertility potential of infected hosts. Furthermore, we explore the probability of disease extinction for varying initial sizes of infected hosts and environmental pathogens using a 3D surface and contour plot in Figure 6. This demonstrates the relationship between the two initial sizes and the probability of disease extinction. Finally, Figure 7 illustrates the approximate probability distribution of extinction times for the number of infected individuals under varying initial conditions. It is observed that the extinction time distribution is influenced by the initial values of infected hosts and environmental pathogens: larger initial values generally lead to longer extinction times. Most infections extinguish quickly, but a small number persist for extended periods.

The present study integrates several critical aspects into the formulation of deterministic and stochastic models, including the self-reproduction of the pathogen in the environment, multiple transmission routes, and the pathogen's potential effects on infected host vital rates such as fertility potential and excess mortality. Evaluating the impact of various pathogens on host extinction or decline, as well as the effects of the same pathogen on different host species, is a critical issue in conservation biology. The model framework presented in this manuscript offers a potential approach for comparative analysis to address these topics. Furthermore, the model formulation is still highly simplified. Additional factors should be considered to improve the comprehensiveness of the model. For instance, the seasonal drivers of frog population growth, reproduction, and disease outbreaks, which depend on numerous spatial and temporal factors, are worth exploring. Several seasonal drivers have been proposed in ecological studies, including temperature, rainfall, and habitat conditions [32, 46, 54]. The environmental conditions contributing to outbreaks can differ between habitats. Therefore, it is essential to incorporate these seasonal factors, which are related to population persistence and disease outbreaks, into the model formulation and prediction. Future investigation will focus on deterministic and stochastic models of the frog-pathogen system in a periodic environment. We leave these interesting topics in future investigations.

Acknowledgments

The authors would like to extend our sincere gratitude to two anonymous referees for providing valuable and constructive comments that greatly enhanced the quality of the original manuscript.

Appendix: Proofs of some results in the main text

A. Proof of Proposition 2.1

Proof. Let $\boldsymbol{g} : \mathbb{R}^3_+ \to \mathbb{R}^3$ be the vector field given by the right hand side of system (1), which is obviously Lipschitz continuous on any bounded subset of $\mathbb{R}^3_+$. It follows that a unique solution $(S(t), I(t), B(t))$ through the initial values in $(S(0), I(0), B(0)) \in \mathbb{R}^3_+$ exists for $t \in [0, t_0)$. Furthermore, the following observations hold for $\boldsymbol{u} = (u_1, u_2, u_3) = (S, I, B) \in \mathbb{R}^3_+$: (i) if $u_1 = 0$, then $g_1(u) = \frac{b_N \cdot \eta u_2}{1+\xi_N \cdot \eta u_2} \geq 0$; (ii) if $u_2 = 0$, then $g_2(u) = \kappa u_3 u_1 \geq 0$; and (iii) if $u_3 = 0$, then $g_3(u) = \gamma u_2 \geq 0$. Based on [21] and [57], these observations imply that solutions starting in $\mathbb{R}^3_+$ are still in $\mathbb{R}^3_+$ once they exist. It remains to show that $t_0 = \infty$. To do that, we consider the sum of three variables

$$G(t) = S(t) + I(t) + B(t),$$

which satisfies

$$\frac{\mathrm{d}G(t)}{\mathrm{d}t} \leq \frac{b_N(S(t) + I(t))}{1 + \xi_N(S(t) + I(t))} + \frac{b_B B(t)}{1 + \xi_B B(t)} + \gamma I(t) \leq b_N S(t) + b_B B(t) + (b_N + \gamma)I(t) \leq cG(t)$$

with $c = \max\{b_B, b_N + \gamma\}$. Therefore, $G(t) = S(t) + I(t) + B(t) \leq G(0)e^{ct}$ for all $t \geq 0$, which implies $t_0 = \infty$. The positive invariance of the set Ω can be verified through [57, Remark 5.2.1]. □

B. The local stability of E_{10}

The corresponding Jacobian matrix is

$$J\Big|_{E_{10}} = \begin{bmatrix} \frac{b_N}{(1+\xi_N S_0)^2} - d_N & \frac{b_N \eta}{(1+\xi_N S_0)^2} - \beta S_0 & -\kappa S_0 \\ 0 & \beta S_0 - d_N - \mu & \kappa S_0 \\ 0 & \gamma & b_B - d_B \end{bmatrix}.$$

All eigenvalues of the Jacobian matrix are

$$\lambda_{1,2} = \frac{(a_{11} + a_{22}) \pm \sqrt{(a_{11} - a_{22})^2 + 4a_{12}a_{21}}}{2}, \quad \lambda_3 = \frac{b_N}{(1 + \xi_N S_0)^2} - d_N = d_N\left(\frac{1}{\mathcal{R}_H} - 1\right) < 0,$$

where $a_{11} = \beta S_0 - d_N - \mu$, $a_{12} = \kappa S_0$, $a_{21} = \gamma$ and $a_{22} = b_B - d_B$.

It is easy to see that if $b_B \geq d_B$, then $a_{22} \geq 0$ and $\lambda_1 = \frac{(a_{11}+a_{22})+\sqrt{(a_{11}-a_{22})^2+4a_{12}a_{21}}}{2} > 0$. If $b_B < d_B$ and $\frac{\beta S_0}{d_N+\mu} + \frac{\gamma\kappa S_0}{(d_N+\mu)(d_B-b_B)} < 1$, then $a_{11} < 0$ and $a_{22} < 0$ and

$$a_{12}a_{21} = \gamma\kappa S_0 < (d_N + \mu - \beta S_0)(d_B - b_B) = a_{11}a_{22}.$$

In this case $\lambda_2 = \frac{(a_{11}+a_{22})-\sqrt{(a_{11}-a_{22})^2+4a_{12}a_{21}}}{2} < 0$ and

$$\lambda_1 \;<\; \frac{(a_{11}+a_{22})+\sqrt{(a_{11}-a_{22})^2+4a_{11}a_{22}}}{2} = \frac{(a_{11}+a_{22})+|a_{11}+a_{22}|}{2} = 0.$$

If $b_B < d_B$ and $\frac{\beta S_0}{d_N+\mu} + \frac{\gamma\kappa S_0}{(d_N+\mu)(d_B-b_B)} > 1$, then

$$a_{12}a_{21} = \gamma\kappa S_0 > (d_N + \mu - \beta S_0)(d_B - b_B) = a_{11}a_{22}.$$

In this case,

$$\lambda_1 \;>\; \frac{(a_{11}+a_{22})+\sqrt{(a_{11}-a_{22})^2+4a_{11}a_{22}}}{2} = \frac{(a_{11}+a_{22})+|a_{11}+a_{22}|}{2} = 0.$$

In summary, the statements hold.

C. Proof of Proposition 2.4

Proof. Define an auxiliary matrix

$$M(\epsilon) = \begin{bmatrix} \beta(S_0+\epsilon) - d_N - \mu & \kappa(S_0+\epsilon) \\ \gamma & b_B - d_B \end{bmatrix},$$

by perturbating the matrix $M(0) = F - V$ with F and V given in (4). It follows from Theorem 2 in [64] that $s(M(0)) < 0$, where $s(M)$ is the spectral bound of the matrix M. By the continuity of spectral bound, there exists small enough $\epsilon > 0$ such that $s(M(\epsilon)) < 0$. Since the total host population size satisfies

$$\frac{\mathrm{d}H(t)}{\mathrm{d}t} \le \frac{b_N H(t)}{1+\xi_N H(t)} - d_N H(t),$$

we have $\limsup_{t\to\infty} S(t) \le \limsup_{t\to\infty} H(t) \le S_0 = \frac{1}{\xi_N}(\frac{b_N}{d_N} - 1)$. Therefore, for $\epsilon > 0$, there exists $t_1 = t(\epsilon) > 0$ such that $S(t) \le S_0 + \epsilon$ for any $t \ge t_1$. Thus for $t \ge t_1$, we have

$$\frac{\mathrm{d}I(t)}{\mathrm{d}t} \le \beta(S_0+\epsilon)I(t) + \kappa(S_0+\epsilon)B(t) - d_N I(t) - \mu I(t),$$
$$\frac{\mathrm{d}B(t)}{\mathrm{d}t} \le b_B B(t) - d_B B(t) + \gamma I(t).$$

Considering the following auxiliary linear system

$$\frac{\mathrm{d}x(t)}{\mathrm{d}t} = M(\epsilon)x(t),$$

where the vector $x(t) = (x_1(t), x_2(t))^{\mathrm{T}}$. We have $\lim_{t\to\infty} x_i(t) = 0$ for $i = 1, 2$ for all initial values since $s(M(\epsilon)) < 0$. Choosing $x(0) = (I(t_1), B(t_1))$, the comparison principle implies that

$$(0,0) \le \lim_{t\to\infty}(I(t), B(t)) \le \lim_{t\to\infty}(x_1(t-t_1), x_2(t-t_1)) = (0,0).$$

Then based on the theory of asymptotically autonomous systems in [73], we have $\lim_{t\to\infty} S(t) = S_0$, which implies that E_{10} is globally asymptotically stable when $\mathcal{R}_H > 1$, $\mathcal{R}_B < 1$ and $\mathcal{R}_0 < 1$. □

D. The local stability of E_{01}

The corresponding Jacobian matrix is

$$J\Big|_{E_{01}} = \begin{bmatrix} b_N - d_N - \kappa B_0 & b_N\eta & 0 \\ \kappa B_0 & -d_N - \mu & 0 \\ 0 & \gamma & \frac{b_B}{(1+\xi_B B_0)^2} - d_B \end{bmatrix}.$$

All eigenvalues of the Jacobian matrix are

$$\lambda_{1,2} = \frac{(a_{11}+a_{22}) \pm \sqrt{(a_{11}-a_{22})^2 + 4a_{12}a_{21}}}{2}, \quad \lambda_3 = \frac{b_B}{(1+\xi_B B_0)^2} - d_B = d_B\left(\frac{1}{\mathcal{R}_B} - 1\right) < 0,$$

where $a_{11} = b_N - d_N - \kappa B_0$, $a_{12} = b_N\eta$, $a_{21} = \kappa B_0$ and $a_{22} = -d_N - \mu < 0$. Then we have

(a) if $a_{11} = b_N - d_N - \kappa B_0 \geq 0$, then

$$\lambda_1 = \frac{(a_{11} + a_{22}) + \sqrt{(a_{11} - a_{22})^2 + 4a_{12}a_{21}}}{2} > \frac{a_{11} + a_{22} + |a_{11} - a_{22}|}{2} = a_{11} \geq 0.$$

The equilibrium is unstable;

(b) if $a_{11} = b_N - d_N - \kappa B_0 < 0$, then

$$\lambda_2 = \frac{(a_{11} + a_{22}) - \sqrt{(a_{11} - a_{22})^2 + 4a_{12}a_{21}}}{2} < 0.$$

Note that $\lambda_1 = \frac{(a_{11}+a_{22})+\sqrt{(a_{11}-a_{22})^2+4a_{12}a_{21}}}{2} < 0$ holds if and only if $(a_{11} + a_{22})^2 > (a_{11} - a_{22})^2 + 4a_{12}a_{21}$, that is, $(d_N + \kappa B_0 - b_N)(d_N + \mu) > \eta b_N \cdot \kappa B_0$. Then we discuss the following scenarios:

(bi) if $d_N \geq b_N$, then $(d_N + \kappa B_0 - b_N)(d_N + \mu) \geq \kappa B_0(d_N + \mu) > \eta b_N \cdot \kappa B_0$ since $\eta \leq 1$. Therefore, $\lambda_1 < 0$;

(bii) if $d_N < b_N$ and $d_N + \kappa B_0 > b_N$, namely $d_N < b_N < d_N + \kappa B_0$, then $\lambda_1 < 0$ holds if and only if $b_N < \frac{(d_N+\kappa B_0)(d_N+\mu)}{\eta\kappa B_0+d_N+\mu}$.

Note that $\frac{(d_N+\kappa B_0)(d_N+\mu)}{\eta\kappa B_0+d_N+\mu} < d_N + \kappa B_0$. In summary, the statements hold.

E. Proof of Proposition 2.5

Proof. The first two cases can immediately be obtained by applying Remark 2.1 and Proposition 2.4. Suppose $\mathcal{R}_B > 1$ and $d_N < b_N < \frac{(d_N+\kappa B_0)(d_N+\mu)}{\eta\kappa B_0+d_N+\mu}$, we can also show that the positive equilibrium does not exists as follows. Let $E^* = (S^*, I^*, B^*)$ be a positive equilibrium, we claim that $B^* > B_0$. Suppose not, then $B^* \leq B_0$, and

$$\frac{b_B B^*}{1 + \xi_B B^*} - d_B B^* + \gamma I^* \geq \left(\frac{b_B}{1 + \xi_B B_0} - d_B \right) B^* + \gamma I^* = \gamma I^* > 0,$$

contradicting to the fact that E^* is an equilibrium. Moreover, we have

$$\begin{aligned} &\frac{b_N}{1 + \xi_N \cdot (S^* + \eta I^*)}(S^* + \eta I^*) - d_N S^* - d_N I^* - \mu I^* = 0, \\ &\kappa \cdot B^* \cdot S^* + \beta \cdot \frac{S^* \cdot I^*}{1 + \alpha I^*} - d_N I^* - \mu I^* = 0. \end{aligned} \tag{10}$$

The second equation of (10) implies that $S^* < \frac{d_N+\mu}{\kappa \cdot B^*} I^*$. Therefore,

$$\begin{aligned} &\frac{b_N}{1 + \xi_N(S^* + \eta I^*)}(S^* + \eta I^*) - d_N S^* - d_N I^* - \mu I^* \\ &< b_N(S^* + \eta I^*) - d_N S^* - d_N I^* - \mu I^* \\ &< (b_N - d_N)\frac{d_N + \mu}{\kappa B^*} I^* + b_N \eta I^* - d_N I^* - \mu I^* \\ &< (b_N - d_N)\frac{d_N + \mu}{\kappa B_0} I^* + b_N \eta I^* - d_N I^* - \mu I^* \\ &= [(b_N - d_N)(d_N + \mu) + (b_N \eta - d_N - \mu)(\kappa B_0)] \frac{I^*}{\kappa \cdot B_0} \\ &< \left[\left(\frac{(d_N + \kappa B_0)(d_N + \mu)}{\eta\kappa B_0 + d_N + \mu} - d_N \right)(d_N + \mu) + \left(\frac{(d_N + \kappa B_0)(d_N + \mu)}{\eta\kappa B_0 + d_N + \mu}\eta - d_N - \mu \right)(\kappa B_0) \right] \frac{I^*}{\kappa \cdot B_0} \\ &= 0 \end{aligned}$$

contradicting to the first equation of (10). □

F. Proof of Proposition 2.6

Proof. The existence of a positive equilibrium, (S^*, I^*, B^*), for the system (1) is obtained as a result of the disease persistence (Theorem 2.1 and Theorem 2.2) [72]. We aim to establish the uniqueness of the positive equilibrium. It is easy to see that

$$I^* = \frac{d_B B^*}{\gamma} - \frac{b_B B^*}{\gamma(1+\xi_B B^*)} \text{ and } S^* = \frac{(d_N+\mu)I^*}{\frac{\beta I^*}{1+\alpha I^*} + \kappa B^*}.$$

Assume that there are two positive equilibria (S_1^*, I_1^*, B_1^*) and (S_2^*, I_2^*, B_2^*). Without loss of generality, we assume that $I_1^* > I_2^*$. Then there must be $0 < m < 1$ such that $I_2^* = mI_1^*$. It follows from the last equation of system (1) that

$$(d_B - f_2(B)) \cdot B = \gamma \cdot I > 0,$$

which implies that $d_B > f_2(B)$. Since $\gamma I_2^* < \gamma I_1^*$, we have

$$d_B \cdot B_2^* - f_2(B_2^*) \cdot B_2^* < d_B \cdot B_1^* - f_2(B_1^*) \cdot B_1,$$

which implies that

$$\begin{aligned} d_B \cdot (B_1^* - B_2^*) &> f_2(B_1^*) \cdot B_1^* - f_2(B_2^*) \cdot B_2^* \\ &= f_2(B_1^*) \cdot B_1^* - f_2(B_1^*) \cdot B_2^* + f_2(B_1^*) \cdot B_2^* - f_2(B_2^*) \cdot B_2^* \\ &= f_2(B_1^*)(B_1^* - B_2^*) + (f_2(B_1^*) - f_2(B_2^*))B_2^*. \end{aligned}$$

It follows that

$$(d_B - f_2(B_1^*)) \cdot (B_1^* - B_2^*) > (f_2(B_1^*) - f_2(B_2^*))B_2^*. \tag{11}$$

Note that $d_B - f_2(B_1^*) > 0$. If $B_1^* \leq B_2^*$, then the left hand side of the inequality (11) is non-positive, while the right hand side is non-negative since $f_2(B_1^*) \geq f_2(B_2^*)$. This contradicts the inequality (11). Thus we obtain $B_1^* > B_2^*$.

Moreover, since $d_B - f_2(B_2^*) > 0$, $f_2(B_2^*) > f_2(B_1^*)$ and $d_B - f_2(B_1^*) > 0$, we have

$$(d_B - f_2(B_1^*)) \cdot B_1^* = \rho I_1^* = \frac{1}{m}\rho I_2^* = \frac{1}{m}(d_B - f_2(B_2^*)B_2^*) < \frac{1}{m}((d_B - f_2(B_1^*))B_2^*),$$

which implies that $B_1^* < \frac{1}{m}B_2^*$. That is, $mB_1^* < B_2^* < B_1^*$.

According to the second equation of system (1), we have

$$\kappa \cdot B \cdot S + \beta \cdot \frac{S \cdot I}{1+\alpha I} = (d_N + \mu)I,$$

that is

$$S = \frac{d_N + \mu}{\frac{\kappa B}{I} + \frac{\beta}{1+\alpha I}}.$$

Hence,

$$S_2^* = \frac{d_N + \mu}{\frac{\kappa B_2^*}{I_2^*} + \frac{\beta}{1+\alpha I_2^*}} < \frac{d_N + \mu}{\frac{\kappa B_1^*}{I_1^*} + \frac{\beta}{1+\alpha I_1^*}} = S_1^*.$$

Moreover,

$$\begin{aligned} S_2^* &= \frac{d_N+\mu}{\frac{\kappa B_2^*}{I_2^*}+\frac{\beta}{1+\alpha I_2^*}} = \frac{d_N+\mu}{\frac{\kappa B_2^*}{mI_1^*}+\frac{\beta}{1+\alpha m I_1^*}} \\ &> \frac{d_N+\mu}{\frac{\kappa B_1^*}{mI_1^*}+\frac{\beta}{m(1+\alpha I_1^*)}} = m\frac{d_N+\mu}{\frac{\kappa B_1^*}{I_1^*}+\frac{\beta}{1+\alpha I_1^*}} = mS_1^*. \end{aligned}$$

Hence, we conclude that $mS_1^* < S_2^* < S_1^*$, $mI_1^* = I_2^* < I_1^*$ and $mB_1^* < B_2^* < B_1^*$.

Next, we need to make sure that the equilibrium satisfies the first equation of system (1). Hence,

$$\begin{aligned} &m(f_1(S_1^*+\eta I_1^*)(S_1^*+\eta I_1^*) - d_N S_1^*) = (d_N+\mu)mI_1^* \\ &= (d_N+\mu)I_2^* = f_1(S_2^*+\eta I_2^*)(S_2^*+\eta I_2^*) - d_N S_2^*. \end{aligned} \tag{12}$$

Therefore, we have

$$m(f_1(S_1^*+\eta I_1^*)(S_1^*+\eta I_1^*) - d_N S_1^*) - d_N\eta I_2^* = f_1(S_2^*+\eta I_2^*)(S_2^*+\eta I_2^*) - d_N S_2^* - d_N\eta I_2^*$$

and thus,

$$m(f_1(S_1^*+\eta I_1^*)(S_1^*+\eta I_1^*) - d_N (S_1^*+\eta I_1^*)) = f_1(S_2^*+\eta I_2^*)(S_2^*+\eta I_2^*) - d_N (S_2^*+\eta I_2^*).$$

For any positive solution (S, I, B), we have

$$f_1(S+\eta I)(S+\eta I) - d_N S - d_N I - \mu I = 0,$$

which implies

$$f_1(S+\eta I)(S+\eta I) = d_N(S+I) + \mu I > d_N(S+I) > d_N(S+\eta I).$$

Therefore,

$$f_1(S+\eta I) > d_N.$$

However, we also have

$$\begin{aligned} &m(f_1(S_1^*+\eta I_1^*)(S_1^*+\eta I_1^*) - d_N(S_1^*+\eta I_1^*)) \\ <&f_1(S_2^*+\eta I_2^*)(mS_1^*+m\eta I_1^*) - d_N(mS_1^*+m\eta I_1^*) \\ =&(f_1(S_2^*+\eta I_2^*) - d_N)(mS_1^*+m\eta I_1^*) \\ <&(f_1(S_2^*+\eta I_2^*) - d_N)(S_2^*+\eta I_2^*), \end{aligned}$$

which contradicts equation (12). Therefore, the positive equilibrium must be unique. □

G. Proof of Theorem 2.1

Proof. Let

$$\begin{aligned} &X_0 := \{x = (x_1, x_2, x_3) \in \mathbb{R}_+^3 : x_2 > 0 \text{ and } x_3 > 0\} \\ &\text{and } \partial X_0 := \mathbb{R}_+^3 \setminus X_0 = \{x \in \mathbb{R}_+^3 : x_2 = 0 \text{ or } x_3 = 0\}. \end{aligned}$$

Clearly, X_0 is an open set relative to $\mathbb{R}_+^3$. For any solution of system (1) through the initial value x, define the solution map $\Phi_t(x) = (S(t;x), I(t;x), B(t;x))$ and period-1 solution map $P = \Phi_1$. It is easy to see that $\Phi_t(X_0) \subset X_0$, $\forall t \geq 0$.

Since the total population size $H(t) = S(t) + I(t)$ satisfies

$$\frac{\mathrm{d}H(t)}{\mathrm{d}t} \leq \frac{b_N H(t)}{1 + \xi_N H(t)} - d_N H(t).$$

We have $\limsup_{t\to\infty}(S(t) + I(t)) = S_0$. Hence for any $\epsilon > 0$, there exists $t_0 > 0$ such that $S(t) + I(t) \leq S_0 + \epsilon$ when $t > t_0$. Therefore, we have

$$\frac{\mathrm{d}B(t)}{\mathrm{d}t} = \frac{b_B B(t)}{1 + \xi_B B(t)} - d_B B(t) + \gamma I(t) \leq \frac{b_B B(t)}{1 + \xi_B B(t)} - d_B B(t) + \gamma(S_0 + \epsilon).$$

Since the equation

$$\frac{\mathrm{d}B(t)}{\mathrm{d}t} = \frac{b_B B(t)}{1 + \xi_B B(t)} - d_B B(t) + \gamma(S_0 + \epsilon)$$

admits a globally asymptotically stable equilibrium

$$\hat{B} = \frac{-(d_B - \gamma\xi_B(S_0 + \epsilon) - b_B) + \sqrt{(d_B - \gamma\xi_B(S_0 + \epsilon) - b_B)^2 + 4d_B\xi_B\gamma(S_0 + \epsilon)}}{2d_B\xi_B}.$$

We have $\limsup_{t\to\infty} B(t) = \hat{B}$. Therefore, $P : \mathbb{R}^3_+ \to \mathbb{R}^3_+$ is point dissipative. It then follows from Theorem 2.9 in [41] that P admits a global attractor in $\mathbb{R}^3_+$. Next we prove that P is uniformly persistent with respect to $(X_0, \partial X_0)$.

Let $M_1 := \{(0, 0, 0)\}$ and $M_2 := \{(S_0, 0, 0)\}$. Since $\lim_{x\to M_1}(\Phi_t(x) - M_1) = 0$ uniformly for $t \in [0, 1]$, for any ε_1, there exists δ_1 such that if $\| x - M_1 \| \leq \delta_1$,

$$\| \Phi_t(x) - M_1 \| \leq \varepsilon_1, \ \ \forall t \in [0, 1]. \tag{13}$$

We first claim that $\limsup_{n\to\infty} \| \Phi_n(x) - M_1 \| \geq \delta_1$ for all $x \in X_0$. Suppose, by contradiction, that $\limsup_{n\to\infty} \| \Phi_n(z) - M_1 \| < \delta_1$ for some $z \in X_0$. Then there exists an integer $N_1 \geq 1$ such that $\| \Phi_n(z) - M_1 \| < \delta_1, \forall n \geq N_1$. This implies that for $n \geq N_1$, we have

$$\| (S(n), I(n), B(n)) \| < \delta_1.$$

By (13), we obtain $\| (S(t), I(t), B(t)) \| \leq \varepsilon_1$ and then $|S(t)| \leq \varepsilon_1$, $|I(t)| \leq \varepsilon_1$, $|B(t)| \leq \varepsilon_1$ as $t \geq N_1$. However, when $t > N_1$, solution $S(t)$ through initial value z satisfies

$$\begin{aligned}\frac{\mathrm{d}S(t)}{\mathrm{d}t} &= \frac{b_N(S(t) + \eta I(t))}{1 + \xi_N(S(t) + \eta I(t))} - d_N S(t) - \kappa B(t)S(t) - \frac{\beta S(t)I(t)}{1 + \alpha I(t)} \\ &> \frac{b_N S(t)}{1 + \xi_N S(t)} - d_N S(t) - \kappa\varepsilon_1 S(t) - \beta\varepsilon_1 S(t).\end{aligned}$$

Since $R_H > 1$, there exists $\varepsilon_1 > 0$ such that $b_N - d_N - \kappa\varepsilon_1 - \beta\varepsilon_1 > 0$. By comparison principle, we obtain a contradiction to $|S(t)| \leq \varepsilon_1$ for $t \geq N_1$.

Since $\lim_{x\to M_2}(\Phi_t(x) - M_2) = 0$ uniformly for $t \in [0, 1]$, for any ε_2, there exists δ_2 such that if $\| x - M_2 \| \leq \delta_2$, we have

$$\| \Phi_t(x) - M_2 \| \leq \varepsilon_2, \ \ \forall t \in [0, 1]. \tag{14}$$

Now we claim that $\limsup_{n\to\infty} \| \Phi_n(x) - M_2 \| \geq \delta_2$ for all $x \in X_0$. Assume, by contradiction, that $\limsup_{n\to\infty} \| \Phi_n(z) - M_2 \| < \delta_2$ for some $z \in X_0$. Then there exists an integer $N_2 \geq 1$ such that $\| \Phi_n(z) - M_2 \| < \delta_2$, $\forall n \geq N_2$, which implies that

$$\| (S(n) - S_0, I(n), B(n)) \| < \delta_2.$$

It follows from (14) that $\| (S(t)-S_0, I(t), B(t)) \| \le \varepsilon_2$ and therefore $|S(t)-S_0| \le \varepsilon_2$, $|I(t)| \le \varepsilon_2$, $|B(t)| \le \varepsilon_2$ when $t \ge N_2$. Then for any $t \ge N_2$, we have

$$\begin{aligned} \frac{\mathrm{d}I(t)}{\mathrm{d}t} &\ge \kappa(S_0-\varepsilon_2)B(t) + \frac{\beta(S_0-\varepsilon_2)}{1+\alpha\varepsilon_2} I(t) - d_N I(t) - \mu I(t), \\ \frac{\mathrm{d}B(t)}{\mathrm{d}t} &\ge \frac{b_B}{1+\xi_B\varepsilon_2} B(t) + \gamma I(t) - d_B B(t). \end{aligned} \tag{15}$$

Consider the linear system

$$\frac{\mathrm{d}w(t)}{\mathrm{d}t} = M_{\varepsilon_2} w(t), \tag{16}$$

where

$$M_{\varepsilon_2} = \begin{bmatrix} \frac{\beta(S_0-\varepsilon_2)}{1+\alpha\varepsilon_2} - d_N - \mu & \kappa(S_0-\varepsilon_2) \\ \gamma & \frac{b_B}{1+\xi_B\varepsilon_2} - d_B \end{bmatrix}.$$

Since $\mathcal{R}_0 > 1$, it then follows that $r_0 = s(M_0) > 0$ and $\frac{\mathrm{d}w(t)}{\mathrm{d}t} = M_0 w(t)$ is unstable. Then there exists $\varepsilon_2 > 0$ such that $r_{\varepsilon_2} = s(M_{\varepsilon_2})$, the principle eigenvalue of M_{ε_2}, is positive. Therefore, system (16) admits a solution $w(t) = e^{r_{\varepsilon_2} t} w(0)$ with appropriate positive initial value $w(0)$. On the other hand, for a specific $(I(N_2), B(N_2)) > 0$, there exists δ_3 such that $(I(N_2), B(N_2)) > \delta_3 w(0)$. Based on (15) and comparison principle, when $t \ge N_2$, we have

$$(I(t), B(t)) > \delta_3 e^{r_{\varepsilon_2}(t-N_2)} w(0),$$

which implies that $I(t)$ and $B(t)$ go to infinity, contradicting to the boundedness of solutions.

Define

$$\begin{aligned} M_\partial &:= \{x \in \partial X_0 : P^n(x) \in \partial X_0, n \ge 0\}, \\ D_1 &:= \{x \in \mathbb{R}^3_+ : x_2 = 0 \text{ and } x_3 = 0\}, \\ D_2 &:= \{x \in \mathbb{R}^3_+ : x_1 = 0 \text{ and } x_2 = 0\}. \end{aligned}$$

Then we claim that $M_\partial = D_1 \cup D_2$. We first prove that $D_1 \cup D_2 \subset M_\partial$. For any $x \in D_1$, the second and third equations of system (1) show that $I(t;x) = 0$ and $B(t;x) = 0$ for all $t \ge 0$. Hence $x \in M_\partial$ and $D_1 \subset M_\partial$. For any $x \in D_2$, then it follows from the first and second equations of system (1) that $S(t;x) = 0$ and $I(t;x) = 0$ for all $t \ge 0$. Hence $x \in M_\partial$ and $D_2 \subset M_\partial$. Now it remains to show that $M_\partial \subset D_1 \cup D_2$. For any $x \in M_\partial$, $P^n(x) \in \partial X_0$, that is, $I(n;x) = 0$ or $B(n;x) = 0$ for all $n \ge 0$. Then there are two cases:

(i) If $I(n;x) = 0$ for all $n \ge 0$, it then follows from the second equation of system (1) that $B(n;x) = 0$ and $S(n;x) = 0$. Hence we must have $x_1 = 0$ and $x_3 = 0$. Moreover, $x_2 = 0$. Therefore $x \in D_1 \cup D_2$.

(ii) If $B(n;x) = 0$ for all $n \ge 0$, then based on the third equation of system (1), $I(n;x) = 0$ for all $n \ge 0$. Then we have $x_2 = 0$ and $x_3 = 0$.

It is easy to see that for any $x \in D_1 \cup D_2$, we have $\lim_{t\to\infty}(S(t;x), I(t;x), B(t;x)) = (0,0,0)$ or $\lim_{t\to\infty}(S(t;x), I(t;x), B(t;x)) = (S_0, 0, 0)$. Based on the above arguments, we conclude that condition (C_2) in Theorem 1.3.1 of [73] holds. It then follows that M_1 and M_2 are disjoint, compact and isolated invariant sets for P in M_∂, and no subset of $\{M_1, M_2\}$ forms a cycle in M_∂. This implies that M_1 and M_2 are isolated invariant sets for P in $\mathbb{R}^3_+$, and $W^s(M_i) \cap X_0 = \emptyset$, $\forall i = 1, 2$, where $W^s(M_i)$ is the stable set of M_i for P.

According to the acyclicity theorem on uniform persistence for maps [73], it follows that $P : \mathbb{R}^3_+ \to \mathbb{R}^3_+$ is uniformly persistent with respect to X_0. Thus the semiflow $\Phi_t : \mathbb{R}^3_+ \to \mathbb{R}^3_+$ is also uniformly persistent with respect to X_0.

□

H. Proof of Theorem 2.2

Proof. The proof is similar to that of Theorem 2.1, with different disjoint, compact and isolated invariant sets for P in M_∂. In addition to M_1, M_2 in the proof of Theorem 2.1, there is an additional compact and isolated invariant set

$$M_3 = \{(0, 0, B_0)\}.$$

Adapting the similar arguments in Theorem 2.1, it suffices to show that $W^s(M_i) \cap X_0 = \emptyset, \forall i = 1, 2, 3$, where $W^s(M_i)$ is the stable set of M_i for P.

We will use the same notations as those in the proof of Theorem 2.1, and first claim that $\limsup_{n\to\infty} \| \Phi_n(x) - M_i \| \geq B_0$ for all $x \in X_0$, and $i = 1, 2$. In fact, based on the third equation of system (1), we have

$$\frac{\mathrm{d}B(t)}{\mathrm{d}t} \geq \frac{b_B B(t)}{1 + \xi_B B(t)} - d_B B(t).$$

The comparisonal principle and Proposition 2.3 imply that

$$\liminf_{t\to\infty} B(t) \geq B_0$$

and hence this claim holds.

Since $\mathcal{R}_B > 1$ and $b_N > \frac{(d_N+\kappa B_0)(d_N+\mu)}{\eta\kappa B_0+d_N+\mu}$, the arguments for the Jacobian matrix (17) shows that it is unstable. Then there exists $\varepsilon_3 > 0$ such that $r_{\varepsilon_3} = s(M_{\varepsilon_3})$, the principle eigenvalue of the perturbed matrix with parameter ε_3

$$M_{\varepsilon_3} = \begin{bmatrix} \frac{b_N}{1+(1+\eta)\xi_N\varepsilon_3} - d_N - \kappa(B_0 + \varepsilon_3) - \beta\varepsilon_3 & \frac{b_N}{1+(1+\eta)\xi_N\varepsilon_3}\eta \\ \kappa(B_0 - \varepsilon_3) & -d_N - \mu \end{bmatrix} \tag{17}$$

is positive. Since $\lim_{x\to M_3} (\Phi_t(x) - M_3) = 0$ uniformly for $t \in [0, 1]$, for any ε_3, there exists δ_3 such that if $\| x - M_3 \| \leq \delta_3$, we have

$$\| \Phi_t(x) - M_3 \| \leq \varepsilon_3, \quad \forall t \in [0, 1]. \tag{18}$$

Now we claim that $\limsup_{n\to\infty} \| \Phi_n(x) - M_3 \| \geq \delta_3$ for all $x \in X_0$. Assume, by contradiction, that $\limsup_{n\to\infty} \| \Phi_n(z) - M_3 \| < \delta_3$ for some $z \in X_0$. Then there exists an integer $N_3 \geq 1$ such that $\| \Phi_n(z) - M_3 \| < \delta_3, \ \forall n \geq N_3$, which implies that

$$\| (S(n), I(n), (B(n) - B_0)) \| < \delta_3.$$

It follows from (18) that $\| (S(t), I(t), B(t) - B_0) \| \leq \varepsilon_3$ and therefore $S(t) \leq \varepsilon_3$, $I(t) \leq \varepsilon_3$, $|B(t) - B_0| \leq \varepsilon_3$ when $t \geq N_2$. Then for any $t \geq N_3$, we have

$$\begin{aligned} \frac{\mathrm{d}S(t)}{\mathrm{d}t} &\geq \frac{b_N(S(t) + \eta I(t))}{1 + \xi_N(1+\eta)\varepsilon_3} - d_N S(t) - \kappa(B_0 + \varepsilon_3)S(t) - \beta\varepsilon_3 S(t), \\ \frac{\mathrm{d}I(t)}{\mathrm{d}t} &\geq \kappa(B_0 - \varepsilon_3)S(t) - (d_N + \mu)I(t). \end{aligned}$$

Similar to the arguments in the proof of Theorem 2.1, we can conclude that $S(t)$ and $I(t)$ go to infinity, contradicting to the boundedness of solutions. This completes the proof. □

I. Proof of Proposition 2.7

Proof. We assume that the pathogens cannot reproduce by themselves, namely $b_B = 0$. Then the third equation of system (1) can be reduced to

$$\frac{\mathrm{d}B(t)}{\mathrm{d}t} = -d_B B(t) + \gamma I(t).$$

Assume that there exists a specific solution $(S(t), I(t), B(t))$ such that $\lim_{t\to\infty}(S(t)+I(t)) = 0$. Then for any $\epsilon_1 > 0$, there exists $t_1 > 0$ such that $S(t) + I(t) < \epsilon_1$ for $t > t_1$. Since $\frac{\mathrm{d}B(t)}{\mathrm{d}t} = -d_B B(t) + \gamma I(t) \leq -d_B B(t) + \gamma \epsilon_1, \ \ \forall t > t_1$, then

$$B(t) \leq B(t_1)e^{-d_B(t-t_1)} + \frac{\gamma\epsilon_1}{d_B}(1 - e^{-d_B(t-t_1)}).$$

Hence, there exist some $t_2 > t_1$ such that

$$B(t) \leq \epsilon_1 + \frac{\gamma\epsilon_1}{d_B} = \left(1 + \frac{\gamma}{d_B}\right)\epsilon_1 \text{ when } t > t_2.$$

It follows that when $t > t_2$, we have

$$\begin{aligned}
\frac{\mathrm{d}S(t)}{\mathrm{d}t} &= f_1(S(t) + \eta I(t))(S(t) + \eta I(t)) - d_N S(t) - \kappa B(t)S(t) - \beta\frac{S(t)I(t)}{1 + \alpha I(t)} \\
&\geq f_1(S(t))S(t) - \left(d_N + \kappa\left(1 + \frac{\gamma}{d_B}\right)\epsilon_1 + \beta\epsilon_1\right)S(t) \\
&= \frac{b_N S(t)}{1 + \xi_N S(t)} - \left(d_N + \kappa\left(1 + \frac{\gamma}{d_B}\right)\epsilon_1 + \beta\epsilon_1\right)S(t).
\end{aligned}$$

Then we can choose $\epsilon_1 > 0$ small enough such that $b_N > d_N + \kappa(1 + \frac{\gamma}{d_B})\epsilon_1 + \beta\epsilon_1$. Assume that $\widetilde{S}(t)$ is the solution to the following equation

$$\frac{\mathrm{d}\widetilde{S}(t)}{\mathrm{d}t} = \frac{b_N \widetilde{S}(t)}{1 + \xi_N \widetilde{S}(t)} - \left(d_N + \kappa\left(1 + \frac{\gamma}{d_B}\right)\epsilon_1 + \beta\epsilon_1\right)\widetilde{S}(t)$$

with $\widetilde{S}(t_2) = S(t_2) > 0$. According to similar arguments in Proposition 2.2, we have

$$\lim_{t\to\infty}\widetilde{S}(t) = \frac{1}{\xi_N}\left(\frac{b_N}{d_N + \kappa(1 + \frac{\gamma}{d_B})\epsilon_1 + \beta\epsilon_1} - 1\right).$$

On the other hand, there is $S(t) \geq \widetilde{S}(t)$ when $t \geq t_2$. Therefore, this contradicts the assumption $\lim_{t\to\infty}(S(t) + I(t)) = 0$. □

CRediT authorship contribution statement

Bei Sun: Methodology, simulation and writing. **Daozhou Gao:** Methodology and reviewing. **Xueying Wang:** Methodology and reviewing. **Yijun Lou:** Conceptualization, methodology and writing.

References

[1] Ackleh, A. S., Carter, J., Chellamuthu, V. K., Ma, B. (2016). A model for the interaction of frog population dynamics with *Batrachochytrium dendrobatidis*, *Janthinobacterium lividum* and temperature and its implication for chytridiomycosis management. Ecological Modelling, 320, 158-169.

[2] Aïnseba, B. E., Benosman, C., Magal, P. (2010). A model for ovine brucellosis incorporating direct and indirect transmission. Journal of Biological Dynamics, 4(1), 2-11.

[3] Allen, L. J. (2010). An introduction to stochastic processes with applications to biology. Boca Raton, FL: CRC press.
[4] Allen, L. J. (2015). Stochastic population and epidemic models. Cham, Switzerland: Springer.
[5] Allen, L. J., van den Driessche, P. (2013). Relations between deterministic and stochastic thresholds for disease extinction in continuous-and discrete-time infectious disease models. Mathematical Biosciences, 243(1), 99-108.
[6] Allen, L. J., Wang, X. (2021). Stochastic models of infectious diseases in a periodic environment with application to cholera epidemics. Journal of Mathematical Biology, 82(6), 48.
[7] Arntzen, J. W., Abrahams, C., Meilink, W. R., Iosif, R., Zuiderwijk, A. (2017). Amphibian decline, pond loss and reduced population connectivity under agricultural intensification over a 38 year period. Biodiversity and Conservation, 26, 1411-1430.
[8] Athreya K. B., Ney P.E. (1972). Branching Processes. New York: Springer.
[9] Bahram, M., Netherway, T. (2022). Fungi as mediators linking organisms and ecosystems. FEMS Microbiology Reviews, 46(2), fuab058.
[10] Bartlett, M. S. (1961). Monte Carlo studies in ecology and epidemiology. In: Proceedings of the Fourth Berkeley Symposium on Mathematical Statistics and Probability. UK: University of California Press London, 4, 39-55.
[11] Boots, M., Sasaki, A. (2003). Parasite evolution and extinctions. Ecology Letters, 6(3), 176-182.
[12] Brannelly, L. A., McCallum, H. I., Grogan, L. F., Briggs, C. J., Ribas, M. P., Hollanders, M., Sasso, T., Lopez, F. M., Newell, D. A., Kilpatrick, A. M. (2021). Mechanisms underlying host persistence following amphibian disease emergence determine appropriate management strategies. Ecology Letters, 24(1), 130-148.
[13] Briggs, C. J., Knapp, R. A., Vredenburg, V. T. (2010). Enzootic and epizootic dynamics of the chytrid fungal pathogen of amphibians. Proceedings of the National Academy of Sciences, 107(21), 9695-9700.
[14] Cheng, Y., Wang, J., Yang, X. (2012). On the global stability of a generalized cholera epidemiological model. Journal of Biological Dynamics, 6(2), 1088-1104.
[15] Codeço, C. T. (2001). Endemic and epidemic dynamics of cholera: the role of the aquatic reservoir. BMC Infectious Diseases, 1(1), 1-14.
[16] Collins, J. P. (2010). Amphibian decline and extinction: what we know and what we need to learn. Diseases of Aquatic Organisms, 92(2-3), 93-99.
[17] De Castro, F., Bolker, B. (2005). Mechanisms of disease-induced extinction. Ecology Letters, 8(1), 117-126.
[18] Dorman, K. S., Sinsheimer, J. S., Lange, K. (2004). In the garden of branching processes. SIAM review, 46(2), 202-229.
[19] Drawert, B., Griesemer, M., Petzold, L. R., Briggs, C. J. (2017). Using stochastic epidemiological models to evaluate conservation strategies for endangered amphibians. Journal of the Royal Society Interface, 14(133), 20170480.
[20] Dunne, J. A., Williams, R. J., Martinez, N. D. (2002). Network structure and biodiversity loss in food webs: robustness increases with connectance. Ecology Letters, 5(4), 558-567.
[21] Fan, G., Lou, Y., Thieme, H. R., Wu, J. (2015). Stability and persistence in ODE modelsfor populations with many stages. Mathematical Biosciences and Engineering, 12(4), 661-686.
[22] Gamża, A. M., Hagenaars, T. J., Koene, M. G., De Jong, M. C. (2023). Combining a parsimonious mathematical model with infection data from tailor-made experiments to understand environmental transmission. Scientific Reports, 13(1), 12986.
[23] Gao, S., Chen, L., Sun, L. (2005). Dynamic complexities in a seasonal prevention epidemic model with birth pulses. Chaos, Solitons & Fractals, 26(4), 1171-1181.
[24] Garira, W., Maregere, B. (2023). The transmission mechanism theory of disease dynamics: Its aims, assumptions and limitations. Infectious Disease Modelling, 8(1), 122-144.
[25] Geng, Y., Lutscher, F. (2021). Competitive coexistence of seasonal breeders. Journal of Mathematical Biology, 83, 1-35.
[26] Ghosh, M., Chandra, P., Sinha, P., Shukla, J. B. (2004). Modelling the spread of carrier-dependent infectious diseases with environmental effect. Applied Mathematics and Computation, 152(2), 385-402.
[27] Grant, E. H. C., Miller, D. A., Schmidt, B. R., Adams, M. J., Amburgey, S. M., Chambert, T., Cruickshank, S. S., et al (2016). Quantitative evidence for the effects of multiple drivers on continental-scale amphibian declines. Scientific reports, 6(1), 25625.
[28] Grogan, L. F., Skerratt, L. F., Berger, L., Cashins, S. D., Trengove, R. D., Gummer, J. P. (2018). Chytridiomycosis causes catastrophic organism-wide metabolic dysregulation including profound failure of cellular energy pathways. Scientific Reports, 8(1), 8188.
[29] Hollanders, M., Grogan, L. F., Nock, C. J., McCallum, H. I., Newell, D. A. (2023). Recovered frog populations coexist with endemic Batrachochytrium dendrobatidis despite load-dependent mortality. Ecological Applications, 33(1), e2724.
[30] Hudson, P. J., Rizzoli, A. P., Grenfell, B. T., Heesterbeek, J. A. P., Dobson, A. P editors. (2002). Ecology of Wildlife Diseases. Oxford: Oxford University Press.
[31] Kolby, J. E., Ramirez, S. D., Berger, L., Richards-Hrdlicka, K. L., Jocque, M., Skerratt, L. F. (2015). Terrestrial dispersal and potential environmental transmission of the amphibian chytrid fungus (*Batrachochytrium dendrobatidis*). PLoS One, 10(4), e0125386.
[32] Kupferberg, S. J., Moidu, H., Adams, A. J., Catenazzi, A., Grefsrud, M., Bobzien, S., Leidy, R., Carlson, S. M. (2022). Seasonal drought and its effects on frog population dynamics and amphibian disease in intermittent streams. Ecohydrology, 15(5), e2395.
[33] Lahodny, G. E., Allen, L. J. (2013). Probability of a disease outbreak in stochastic multipatch epidemic models. Bulletin of Mathematical Biology, 75, 1157-1180.
[34] Lanzas, C., Davies, K., Erwin, S., Dawson, D. (2020). On modelling environmentally transmitted pathogens. Interface Focus, 10(1), 20190056.
[35] Liao, S., Wang, J. (2012). Global stability analysis of epidemiological models based on Volterra–Lyapunov stable matrices. Chaos, Solitons & Fractals, 45(7), 966-977.
[36] Li, M., Jin, Z., Sun, G., Zhang, J. (2017). Modeling direct and indirect disease transmission using multi-group model. Journal of Mathematical Analysis and Applications, 446(2), 1292-1309.
[37] Li, M., Pei, X., Zhang, J., Li, L. (2019). Asymptotic analysis of endemic equilibrium to a brucellosis model. Mathematical Biosciences and Engineering, 16(5), 5836-5850.

[38] Lou, Y., Zhao, X.-Q. (2009). Threshold dynamics in a time-delayed periodic SIS epidemic model. Discrete and Continuous Dynamical Systems - Series B, 126(1), 169-186.

[39] Ma, X., Wang, W. (2010). A discrete model of avian influenza with seasonal reproduction and transmission. Journal of Biological Dynamics, 4(3), 296-314.

[40] MacNeil, C., Dick, J. T., Hatcher, M. J., Terry, R. S., Smith, J. E., Dunn, A. M. (2003). Parasite-mediated predation between native and invasive amphipods. Proceedings of the Royal Society of London. Series B: Biological Sciences, 270(1521), 1309-1314.

[41] Magal, P., Zhao, X.-Q. (2005). Global attractors and steady states for uniformly persistent dynamical systems. SIAM Journal on Mathematical Analysis, 37(1), 251-275.

[42] Maity, S., Mandal, P. S. (2022). A comparison of deterministic and stochastic plant-vector-virus models based on probability of disease extinction and outbreak. Bulletin of Mathematical Biology, 84(3), 41.

[43] Malagon, D. A., Melara, L. A., Prosper, O. F., Lenhart, S., Carter, E. D., Fordyce, J. A., Peterson, A. C., Miller, D. L., Gray, M. J. (2020). Host density and habitat structure influence host contact rates and Batrachochytrium salamandrivorans transmission. Scientific Reports, 10(1), 5584.

[44] Maliyoni, M. (2021). Probability of disease extinction or outbreak in a stochastic epidemic model for west nile virus dynamics in birds. Acta Biotheoretica, 69(2), 91-116.

[45] Maliyoni, M., Chirove, F., Gaff, H. D., Govinder, K. S. (2017). A stochastic tick-borne disease model: Exploring the probability of pathogen persistence. Bulletin of Mathematical Biology, 79, 1999-2021.

[46] McCaffery, R., Solonen, A., Crone, E. (2012). Frog population viability under present and future climate conditions: a Bayesian state-space approach. Journal of Animal Ecology, 81(5), 978-985.

[47] Mendelson III J R, Lips K R, Gagliardo R W, et al. (2006). Confronting amphibian declines and extinctions. Science, 313(5783), 48-48.

[48] O'Regan, S. M., Palen, W. J., Anderson, S. C. (2014). Climate warming mediates negative impacts of rapid pond drying for three amphibian species. Ecology, 95(4), 845-855.

[49] Peace, A., O'Regan, S. M., Spatz, J. A., Reilly, P. N., Hill, R. D., Carter, E. D., Wilkes, R. P., Waltzek, T. B., Miller, D. L., Gray, M. J. (2019). A highly invasive chimeric ranavirus can decimate tadpole populations rapidly through multiple transmission pathways. Ecological Modelling, 410, 108777.

[50] Quinn, T. J. (2006). Population dynamics. Encyclopedia of Environmetrics, 3, 1604-1615.

[51] Rachowicz, L. J., Briggs, C. J. (2007). Quantifying the disease transmission function: effects of density on Batrachochytrium dendrobatidis transmission in the mountain yellow-legged frog Rana muscosa. Journal of Animal Ecology, 711-721.

[52] Rosà, R., Pugliese, A., Villani, A., Rizzoli, A. (2003). Individual-based vs. deterministic models for macroparasites: host cycles and extinction. Theoretical Population Biology, 63(4), 295-307.

[53] Roznik, E. A., Sapsford, S. J., Pike, D. A., Schwarzkopf, L., Alford, R. A. (2015). Condition-dependent reproductive effort in frogs infected by a widespread pathogen. Proceedings of the Royal Society B: Biological Sciences, 282(1810), 20150694.

[54] Ruggeri, J., Longo, A. V., Gaiarsa, M. P., Alencar, L. R., Lambertini, C., Leite, D. S., Carvalho-e-Silva, S. P., Zamudio, K. R., Toledo, L. F., Martins, M. (2015). Seasonal variation in population abundance and chytrid infection in stream-dwelling frogs of the Brazilian Atlantic forest. PloS One, 10(7), e0130554.

[55] Scheele, B. C., Pasmans, F., Skerratt, L. F., Berger, L., Martel, A. N., Beukema, W., et al (2019). Amphibian fungal panzootic causes catastrophic and ongoing loss of biodiversity. Science, 363(6434), 1459-1463.

[56] Shea, K., Chesson, P. (2002). Community ecology theory as a framework for biological invasions. Trends in Ecology & Evolution, 17(4), 170-176.

[57] Smith, H. L. (1995). Monotone dynamical systems: an introduction to the theory of competitive and cooperative systems: an introduction to the theory of competitive and cooperative systems. American Mathematical Society, 41.

[58] Smith, M. J., White, A., Sherratt, J. A., Telfer, S., Begon, M., Lambin, X. (2008). Disease effects on reproduction can cause population cycles in seasonal environments. Journal of Animal Ecology, 77(2), 378-389.

[59] Stuart, S. N., Chanson, J. S., Cox, N. A., Young, B. E., Rodrigues, A. S., Fischman, D. L., Waller, R. W. (2004). Status and trends of amphibian declines and extinctions worldwide. Science, 306(5702), 1783-1786.

[60] Sun, G., Li, M., Zhang, J., Zhang, W., Pei, X., Jin, Z. (2020). Transmission dynamics of brucellosis: Mathematical modelling and applications in China. Computational and Structural Biotechnology Journal, 18, 3843-3860.

[61] Tang, S., Cheke, R. A. (2008). Models for integrated pest control and their biological implications. Mathematical Biosciences, 215(1), 115-125.

[62] Tobler, U., Borgula, A., Schmidt, B. R. (2012). Populations of a susceptible amphibian species can grow despite the presence of a pathogenic chytrid fungus. PLoS One, 7(4), e34667.

[63] Toledo, L. F., de Carvalho-E-Silva, S. P., de Carvalho, A. M. P. T., Gasparini, J. L., Baêta, D., Rebouças, R., Haddad, C. F.B., Becker, C. G., Carvalho, T. (2023). A retrospective overview of amphibian declines in Brazil's Atlantic Forest. Biological Conservation, 277, 109845.

[64] van den Driessche, P., Watmough, J. (2002). Reproduction numbers and sub-threshold endemic equilibria for compartmental models of disease transmission. Mathematical Biosciences, 180(1-2), 29-48.

[65] van den Driessche, P., Yakubu, A. A. (2020). Age structured discrete-time disease models with demographic population cycles. Journal of Biological Dynamics, 14(1), 308-331.

[66] van den Driessche, P., Yakubu, A. A. (2019). Disease extinction versus persistence in discrete-time epidemic models. Bulletin of Mathematical Biology, 81(11), 4412-4446.

[67] Wang, J. (2022). Mathematical models for cholera dynamics-A review. Microorganisms, 10(12), 2358.

[68] Wang, J., Liao, S. (2012). A generalized cholera model and epidemic–endemic analysis. Journal of Biological Dynamics, 6(2), 568-589.

[69] Wang, X., Zhao, X.-Q., Wang, J. (2018). A cholera epidemic model in a spatiotemporally heterogeneous environment. Journal of Mathematical Analysis and Applications, 468(2), 893-912.

[70] Xiao, Y., Bowers, R. G., Tang, S. (2009). The effect of delayed host self-regulation on host-pathogen population cycles in forest insects. Journal of Theoretical Biology, 258(2), 240-249.
[71] Yakubu, A. A. (2010). Introduction to Discrete-time Epidemic Models. DIMACS Series in Discrete Mathematics and Theoretical Computer Science, 75, 83-107.
[72] Zhao, X. Q. (2008). Permanence implies the existence of interior periodic solutions for FDEs. International Journal of Qualitative Theory of Differential Equations and Applications, 2(125-137), 17.
[73] Zhao, X.-Q. (2017). Dynamical Systems in Population Biology. New York: Springer.
[74] Zhao, X.-Q., Jing, Z. J. (1996). Global asymptotic behavior in some cooperative systems of functional differential equations. Canadian Applied Mathematics Quarterly, 4(4), 421-444.